

**EXTREMELY LOW FREQUENCY (ELF) SIGNAL
PROCESSING FOR ELECTRIC
BOREHOLE TELEMETRY**

By

FARHAD ESFAHANI

**Bachelor of Science in Electrical Engineering
Oklahoma State University
Stillwater, Oklahoma
1984**

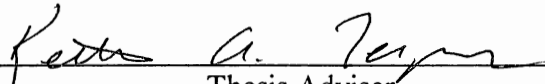
**Master of Science in Electrical Engineering
Oklahoma State University
Stillwater, Oklahoma
1986**

**Submitted to the Faculty of the
Graduate College of the
Oklahoma State University
in partial fulfillment of
the requirements for
the Degree of
DOCTOR OF PHILOSOPHY
December, 1992**

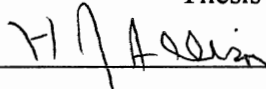
Thesis
1992D
E15e

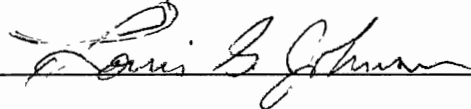
EXTREMELY LOW FREQUENCY(ELF) SIGNAL
PROCESSING FOR ELECTRIC
BOREHOLE TELEMETRY

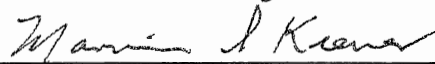
Thesis Approved

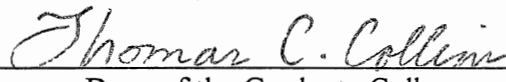


Thesis Adviser









Dean of the Graduate College

ACKNOWLEDGMENTS

I will always be indebted to my parents, Ali and Parivash Esfahani whose constant support and encouragement helped me through hard times and gave me the motivation to continue on.

I will be indebted to my thesis adviser, Keith Teague for his time, help and guidance and to the chairman of my advisory committee, Jack Allison who has been a great inspiration for me since I entered the School of Electrical and Computer Engineering in the University. I also appreciate the time and effort spent by the other members of my committee: Louis Johnson and Marvin Keener.

I greatly appreciate the support of my wife Karen who helped me through by being there for me. To Oddie who provided moral support and believed in me I extend many hugs. I wish to express sincere appreciation to my good friend Mark Richardson for his help, suggestions and proofing of my thesis. And I am especially thankful to the opportunity provided for me by Halliburton Services Company and the Gas Research Institute. This research project was funded partly by the Gas Research Institute

TABLE OF CONTENTS

Chapter	page
I. INTRODUCTION	1
Previous Work	3
Acoustic Systems	3
Wireline Systems	4
Mudpulse Systems	5
Electromagnetic Systems	7
Contributions of This Research	11
Document Overview	13
II. NOISY EARTH	15
Noise Cancellation Using Adaptive Filters	19
Impulsive Noise Cancellation for Low Sample Rate Data	29
III. DIFFERENTIAL PHASE SHIFT KEYED (DPSK) MODULATION/DEMULATION	40
Probability of Error For Optimum DPSK Demodulation System	45
IV. SYSTEM OVERVIEW	51
V. SUMMARY AND CONCLUSIONS	63
Recommended Future Research	66
REFERENCES	67
APPENDIX - NEURAL NETWORKS: INTRODUCTION	71

TABLES

Table	page
1.1 Main Drilling Problems	3

LIST OF FIGURES

Figure	Page
1.1 Through the earth transmitter	10
1.2 Attenuation rate plot for 3Hz signal	12
2.1 Test well data with transmitter at depth of 3000 feet for a stormy day	17
2.2 Test well data with transmitter at depth of 2500 feet for a relatively calm day	18
2.3 Noise Cancellation	20
2.4 ANC	22
2.5 Adaptive noise canceller simulation results	26
2.6 Filtering well data using ANC	27
2.7 Bias removal	28
2.8 60Hz sine wave sampled at 256Hz	32
2.9 Median filter result	32
2.10 Linear estimation method for spike removal	33
2.11 Impulsive noise removal using the proposed method	38
2.12 Proposed filter block diagram	38
2.13 A comparison of different impulse removal filters	39
3.1 Differential encoding	42
3.2 Dpsk Demodulator	42
3.3 Equivalence gate used for differential encoding	43
3.4 Carrier frequency estimation	44
3.5 Optimum dpsk demodulator	45
3.6 Derivation of variance for intermediate variables	49
3.7 Error Probabilities for some digital signaling methods	50
4.1 Antenna arrangement	54
4.2 Current flow directions in the earth	55
4.3 Sample primary input signal spectrum	58
4.4 Sample reference input signal spectrum	59
4.5 Simulated 6Hz signal	60
4.6 EBT Signal Processor	62
A.1 Backpropagation Neural Network Architecture	74
A.2 A Processing Element	74
A.3 Learning Process in a three layer Backpropagation neural network	75

SYMBOLS AND ABBREVIATIONS

- e_n - Induced voltage in antenna n
 e_w - Transmitter voltage
 I_w - Transmitter Current
 I_1 - Current in antenna 1
 I_2 - Current in antenna 2
 R_w - Transmitter antenna resistance
 R_1 - Antenna 1 resistance
 R_2 - Antenna 2 resistance
 $\Phi()$ - Unit step function
 μ - Convergence factor
 N_w - Number of weights in the adaptive noise canceller
 $E\{\}$ - Expectation operator
 ∇_j - Gradient at the jth iteration
 X_j - Reference input vector
 $x(n)$ - A single reference input value
CC - Cross correlation matrix. for reference and primary inputs
R - Reference input correlation matrix
 ϵ_j - Error at the jth iteration
 $erfc(x)$ - Complementary error function = $1 - erf(x)$
 P_E - Probability of Error
 P_r - Probability of
 f_r - Distribution function of random variable r
- ANC - Adaptive Noise Canceller
DPSK - Differential Phase Reversal Keyed
EBT - Electromagnetic Borehole Telemetry
LMS - Least Mean Squared
MWD - Measurement While Drilling
PRK - Phase Reversed Keyed
PSK - Phase Shift Keyed
SNR - Signal to Noise Ratio

CHAPTER I

INTRODUCTION

Being able to receive downhole information while performing operations on an oil or a gas well has always been a highly desired capability for oil and oil service companies. Having real time bottom-hole information at the surface will assist with operations such as drilling, stimulation, and cementing. This type of information can increase accuracy, reduce equipment failure and total operation costs, and most importantly, reduce safety hazards. For example, one of the major safety concerns in drilling has to do with the influx of formation fluids. Real time data telemetry has the potential of giving early warning by measuring and detecting changes in the mud properties down-hole. Having available real time downhole data takes a lot of the guesswork out of crucial decisions on the surface. Also measurements made before any unwanted changes in the borehole will improve data interpretation.

Among all oil well operations, the one which can benefit most significantly from real time bottom-hole data is probably exploratory drilling. One of the important advantages is that early recognition of interesting formations allows formation evaluation under minimum damage conditions. Measurement While Drilling (MWD) data concerning downhole lithology is collected in the earliest and most undamaged borehole conditions. MWD is specially useful for deep and horizontal wells. Down hole measurement will

allow safer, more efficient and more economic drilling of both exploration and production wells. Continuous monitoring of downhole conditions will allow immediate response to potential well-control problems. It will also help eliminate costly drilling interruptions while circulating fluids. Overall it could improve drilling rates anywhere from 5 to 15% [23]. MWD allows for controlling direction and orientation of a well in real time as well as helping in prevention and remedy of most downhole problems. Some of the problems associated with drilling are listed in table 1.1. Current borehole telemetry techniques include use of wirelines, mud-pulse systems and acoustic systems. At present, no commercial acoustic systems exist, mainly because of very high attenuation rates of the acoustic signals travelling along the drill string. Mud pulse systems are the most widely used systems and they are all limited to a few words per minute of data transmission. They can provide information sufficient to save many hours of valuable rig time, however, the wireline technique offers a higher transmission rate than any other type of borehole telemetry system and eliminates the need for a downhole power source. However, because of the expense and cumbersome nature of the equipment, the service companies have not been able to base a competitive service on the technique.

TABLE 1.1
MAIN DRILLING PROBLEMS

-
- _sticking tendencies
 - _inadequate cuttings lift or hole cleaning
 - _wear in bit teeth or cutter
 - _problems with bit bearings
 - _gumbo ballings around bit or stabilizers
 - _formation water influx
 - _excessive fluid loss
-

Acoustic systems

In the 1940's a few companies started research towards a different telemetry system. Most of the work was done independently by these companies but they more or less reached the same conclusion, that an acoustical system would be the most promising borehole telemetry system. In an acoustical system, sound waves are generated and travel through metal drill pipe. Since the rate of attenuation of sound in steel was known to be low, it was assumed that systems could be designed to use the metal wall of the pipes as the transmission channel. However, this turned out to be disappointing.

In 1948 Sun Oil company built a system to study the feasibility of acoustic systems. This telemetry system consisted of a downhole impulsive sound generator and a surface sound receiver designed to receive transmitted sound in three different frequency bands.

The sound generator was battery operated with a motor that wound up a spring and, when released, the spring drove a hammer to deliver a sound impulse to the drill pipe. The results of this study were very disappointing. The attenuation rates were so high that it discouraged any further effort on this type of telemetry system. The conclusion was that an acoustic telemetry system was not feasible within the state-of-the-art existing at that time. Later, it was considered practical to use repeaters to overcome the high attenuation rates.

Today, no commercial acoustical telemetry systems exist, because of the number of repeaters needed along the drill pipe and because of the requirement that a drill pipe must be in the well for the system to operate. A good example of an acoustic system is one invented by W.H. Cox and P.E. Chaney, U.S. Patent No. 4,293,936. In their work, Cox and Chaney have disclosed a band of frequencies at which they obtained minimum attenuation rates for transmission of sound through the wall of a drill pipe but they still require a repeater every 2000 feet.

Wireline systems

Wireline telemetry is one of the most widely used techniques for borehole communications to date. The first commercial system was used with a steering tool for directional drilling. Wireline communication systems are bi-directional communications systems that provide the highest data rates compared with other current methods such as mud pulsing and non-real time systems where a memory recorder is used to collect data. Different methods using wireline borehole telemetry are in current use. One method uses

an armored cable for data transmission, U.S. patent No. 3,707,700 to Lafont. Another uses the same wireline for both delivery of power and communications, U.S. patent No. 4,646,083 to Woods. Other systems include U.S. patent Nos. 4,355,310 to A. B. Beynes, which provides for transmission rates of up to 80KHz and 3,991,611 to J. H. Marsall III and T. M. Harrington, which is similar to digital remote telemetry systems used most commonly in the field of industrial controls and uses a single insulated wire within the hoist cable as the transmission channel.

One problem with wireline systems is the requirement of complete withdrawal of the cable or the making of connections in the cable at the surface each time a new pipe section is added to the drill string. This is a cumbersome and time consuming process. Some other drawbacks of wireline systems are the bulkiness of thousands of feet of cable, the cost of the cable and the fact that the harsh environment they operate in can be very abrasive to the cable itself.

One of the systems uses the drill string as the electric transmission line. The difficulty in such a system lies in reliability of the electrical connection between adjacent interconnected pipes forming the drill string [23] and also in electrical insulation from the surrounding earth. Attempts have been made to embed electrical conductors into the drill pipes. This method is feasible but has proven to be too costly [6].

Mud pulse systems

The most widely used MWD borehole telemetry system is the mud pulsing system. All mud pulse systems use the mud stream inside the drill pipes as the communication channel.

The first mechanical mud pulse system was marketed in 1964 for transmission of directional drilling data [8].

Three different mud pulse methods exist; positive pressure, negative pressure and the mud siren [6],[23]. These are all one directional communication systems. In the positive pressure mud pulse system, a valve at the bottom of the well is opened or closed according to what data is to be transmitted [7]. Valve closure restricts the flow of mud which in turn creates pressure waves in the mud column that are then detected at the surface. This type of system has typical data rates of 0.4 bits per second. In negative pressure systems, a valve opens the flow to the annular space between the drill pipe wall and the borehole [7]. Each time the valve is opened a pressure drop is detected at the surface. Typical data rates for negative pressure systems are about one bit per second.

The fastest communication system utilizing drilling mud as the transmission medium is called the mud siren. A mud siren system is a continuous wave system in which the data is transmitted as a phase shift keyed (PSK) signal [8]. The system consists of two slotted wheels. One is stationary and the other is controlled by a motor and can change direction. The mud flows through both wheels and pressure waves are created by the second moving wheel as it turns. The commercial mud siren system's typical data rate is about one and a half bits per second.

All mud pulse systems are very sensitive to pump noise and to anything else that creates pressure waves, such as shale gumbo balling around the drill bit teeth. Filtering is very difficult because of the broad noise spectrum. The mud pulse systems require continuous fluid flow through the well, which limits the use of such systems to regular

drilling operations. Examples of different mud pulsing systems are shown in U.S. patent nos 4,734,893 to Claycomb, 4,550,392 and 4,699,352 to Mumby, and 4,641,289 to Jurgens. Other systems include U.S. patent nos. 2,759,143 and 2,925,251 to Arps and 3,958,217 to Spinnler which disclose positive pressure pulse systems, U.S. patent nos 2,887,298 to Hampton and 4,078,620 to Westlake which disclose negative pressure pulse systems.

Electromagnetic systems

Currently, no commercially available electromagnetic borehole communications systems exist. Such a system would be a two way communication system using electromagnetic waves in the extremely low frequency (ELF) range of the spectrum. There have been a few proposals for electromagnetic communications in the borehole and none has been very successful.

One such system is disclosed in U S patent No 4,800,385 to Yamazaki, which utilizes a drill string made of magnetic material as the transmission channel. The downhole transmitter antenna is a coil wound on the bottom portion of the drill string. The magnetic flux signal is picked up as an electric signal at a coil fixed around an exposed end of the drill string on the surface. The receiver utilizes a band pass filter to enhance signal-to-noise-ratio (SNR) with no additional noise cancelling system. A few other references disclosing systems using electromagnetic waves are. U S. patent nos 3,967,201 to L. H. Rorden where vertically polarized antennas are used to reduce in the earth atmospheric interference with best results with a parallel well containing the receiving

antenna drilled next to the operating well. Their tests were performed utilizing a 100 watt peak power supply system which is difficult to achieve using batteries; 4,087,781 to M. D. Grossi and R. K. Cross who have not disclosed any particular filtering or noise cancelling methods; and 4,090,135 to A. J. Farstad and C. Fisher Jr. who have used frequency shift keyed (FSK) modulation/demodulation in their system with threshold detection and with low pass filter for SNR enhancement. None of these systems use any type of adaptive filtering methods and none considers the varying noise conditions existing in through-the-earth communications. One factor contributing to their limited commercial success if any may be the interference existing within the frequency band of interest which presents problems when low power transmitters are used. A signal processing system incorporating adaptive noise cancellation that could attenuate the interference within the signal frequency range would be able to increase the signal-to-noise-ratio for better reception. Also an adaptive filtering system can modify its own parameters to adjust to the different noise conditions.

Major benefits of an electromagnetic borehole communication systems are the higher data rates possible and the fact that these systems can be used in any type of well operation. Air drilling, very small diameter downhole, high angle boreholes, higher data rate demands and non-drilling needs such as cementing or stimulation, present a set of conditions that only the electromagnetic system could handle.

An Electromagnetic Borehole Telemetry (EBT) system has been proposed and is under development at Halliburton Services Company. The system will allow transfer of downhole information to the surface under most conditions. It will make possible two

way communications that will enable the operators to actuate or modify the downhole tool mode. Whether drilling, stimulation or cementing is in process, whether fluid is flowing in the well or not, information can be transmitted to the surface. The primary industry benefits of the EBT system are the ability to transmit downhole data to the surface in real time during well operations, lower price than the state-of-the-art wireline conveyed equipment, a hardware configuration that is not operationally restrictive, and a data transmission rate that exceeds existing wireless methods such as mud pulsing.

The EBT system is to operate in either a cased well or in an open hole. The tubing or cable conveyed tool can be lowered into the well to provide real time data at the surface while drilling, stimulation or cementing operations are in progress. The receiver antennas are wire antennas laid out on the ground and connected to the well head at one end and to a ground rod at the other. The length of the antennas are on the order of a few hundred feet. No optimum length has been determined. Figure 1.1 shows a schematic diagram of the antenna arrangement with respect to the well. Because of high attenuation rates and the amount of noise, deep digital filtering and noise cancellation is essential for reliable communications.

There are two classes of noise that affect performance of all electromagnetic borehole communication systems. These are random noises -- atmospheric, telluric, pipe scraping, etc., and coherent noises -- power equipment, power supply, etc. The coherent noise present consists primarily of 60 cycle interference and its harmonics [26]. These are well understood and are relatively simple to filter out. Most of the problems are associated

with the random, impulsive noise created by the power grid switching and by thunderstorms.

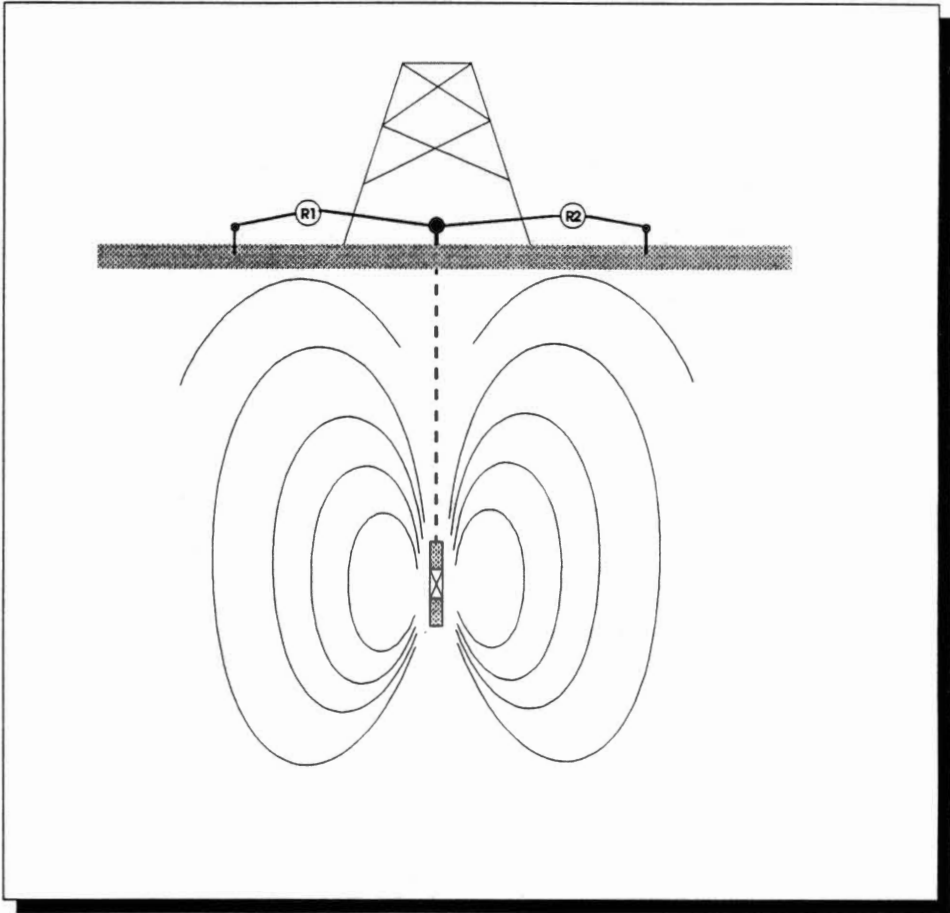


Figure 1.1- Through the earth transmitter

Contributions of this research

Signals received through the earth contain large amounts of both random, time varying noise and non-random noise. Conventional signal processing techniques assume that the signal degradation is a known time-invariant quantity. Experimental data show that the attenuation rate of a 3Hz sine wave transmitted through the casing to the surface is between 8 and 10 db per 1000 feet and when propagating through the earth it is 16 db per 1000 feet. Figure 1.2 shows a plot of data obtained by transmitting a 3Hz signal with the transmitter at different depths in the borehole. A jump in the signal level can be seen where the casing ends and signals start to travel through the earth. However, the attenuation rate through the earth is actually greater. This is an indication of the dependence of the attenuation rates on the randomly changing (with depth) of the formation conductance. The noise in the earth is a time-varying phenomenon that changes for different sites as the earth's lithology changes. A signal processing system is needed that can compensate for these changes and that can provide sufficient noise cancelling to ensure accurate reception of data from the borehole

An adaptive noise cancelling system was designed that takes advantage of the fact that the noise in the ELF band is highly correlated at distances up to a few miles. The adaptive noise canceller uses a reference input that contains a noise source which is highly correlated to the noise in the primary input. The primary input contains the data that needs to be filtered. Also, an impulsive noise removal filter was devised to remove any spikes from the data. The impulsive noise removal system is distinctive in that it will not introduce any undesired effects into low sample rate data, as would be the case with other

techniques, such as median filtering. A minimum error (in terms of bit loss) modulation and demodulation system is used for data transmission using a differential coding scheme that does away with the requirement of a coherent reference. A new method for signal demodulation is presented that takes advantage of neural networks and their pattern recognition ability.

This signal processing scheme results in sufficient SNR improvement that the telemetry tool operates to depths of slightly over 5000 feet at a signal frequency of 3 Hz, without the need for repeaters. The prototype downhole transmitter operates on batteries and delivers an output current of 4 amperes rms. With more powerful power systems, both the depth of operation and the data rate can be increased.

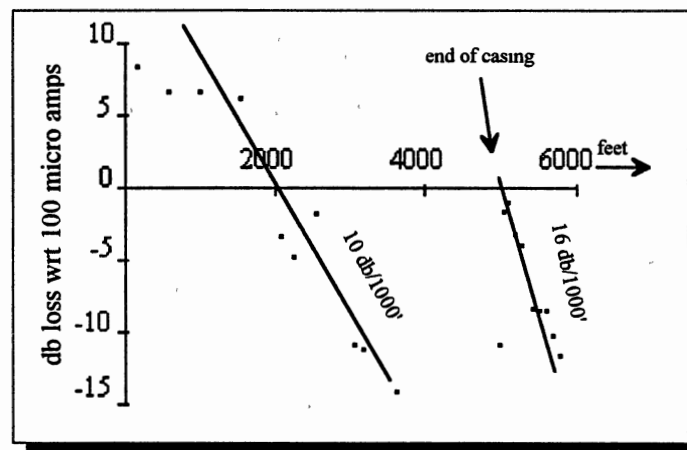


Figure 1.2- Attenuation rate for 3Hz sine wave transmitted from the borehole.

DOCUMENT OVERVIEW

This document contains five chapters. The purpose of this first introductory chapter is to present a general description of the problem of borehole communication systems and to discuss existing systems and to present work done to date on such systems. Contributions of this research and an overview of the entire document are also included. A limited knowledge of communication systems and oil well terminology is presumed for the first two sections.

Chapter 2 describes the noise conditions involved in through-the-earth communications. The time and site-varying characteristics of the noise are explained and filtering methods for removal of the unwanted disturbances are described. Adaptive noise cancellers are shown to provide significant SNR gains. Finally, a method of impulsive noise cancellation is described.

Chapter 3 reviews the concepts of modulation and demodulation and provides a comparison of different techniques. The selection criteria for the particular method used is discussed, together with a calculation of the probability of error for an optimum demodulator. An alternative solution to the classical demodulation methods is presented. The alternative system takes advantage of pattern recognition capabilities of neural networks.

Chapter 4 presents an overview of the proposed system together with results of simulations.

Chapter 5 presents the summary and conclusions of this thesis. The benefits and the limitations of the proposed signal processing system are discussed. This chapter also includes a section on potential future research work.

The last part of the thesis contains the reference section. An appendix is added that contains a concise description of backpropagation neural networks.

CHAPTER II

NOISY EARTH

The primary noise source in the earth is the power grid noise which is responsible for impulsive switching and line noise. The 60Hz and its harmonics have the greatest amplitudes compared to the earth noise floor and any other noise that may exist. Higher frequency interference such as 60Hz and its harmonics can be filtered out relatively easily. But the major concern is with the noise in the extremely low frequency band where the signals of interest are. The EBT system uses the ELF range to transmit data to the surface. The noise present in the ELF band is difficult to characterize and model. Primary origins of ELF noise are believed to be distant thunderstorms [12], high power, low frequency noise travels far and so it is highly correlated at sites apart as much as a few miles. Experimental data collected at a test well during calm atmospheric conditions and during thunderstorm conditions shows this to be true.

The high degree of noise correlation between distant locations makes adaptive noise cancelling a good choice for noise removal. The higher frequency noises can also be removed by the adaptive noise canceller if proper reference is available. A proper reference is one that contains noise which is highly correlated with the noise in the main antenna, while being correlated as little as possible with the signal of interest. An antenna placed a few hundred feet away from a well head will contain almost no signal and will

contain highly correlated noise in both ELF and higher frequency ranges. Data collected from different sites show that the line noise increases as the site falls within the power grid, while the ELF noise power changes slowly as the site location is changed. An interesting observation on data collected at a site near the Halliburton Research Center shows that the noise power is significantly decreased after five o'clock in the evening when most of the electrical systems are shut down.

On stormy days, when there are lightning strikes close to where the antennas are located, a lot of impulsive noise, as well as ELF noise, can be observed at the receiver output. Figure 2.1 shows time and spectrum plots of data collected on a stormy day with the transmitter in the test well at a depth of 3000 feet. Even after all the filtering is done, a significant amount of noise remains in the data due to the high power of noise. The signal-to-noise ratio is very low in such conditions and the signal can not be demodulated successfully. Figure 2.1a shows the spectrum of data before any processing, figures 2.1b and 2.1c show the spectrum of the output of the adaptive filter stage and Figure 2.1d shows the filtered data in the time domain. Figure 2.2 shows the time and spectrum plots of data collected on a calm day with the transmitter at a depth of 2500 feet. The output of the filters is shown in Figure 2.2d, in which a 6 Hz phase reversed keyed signal was transmitted from the borehole. The wave form shown can be successfully demodulated.

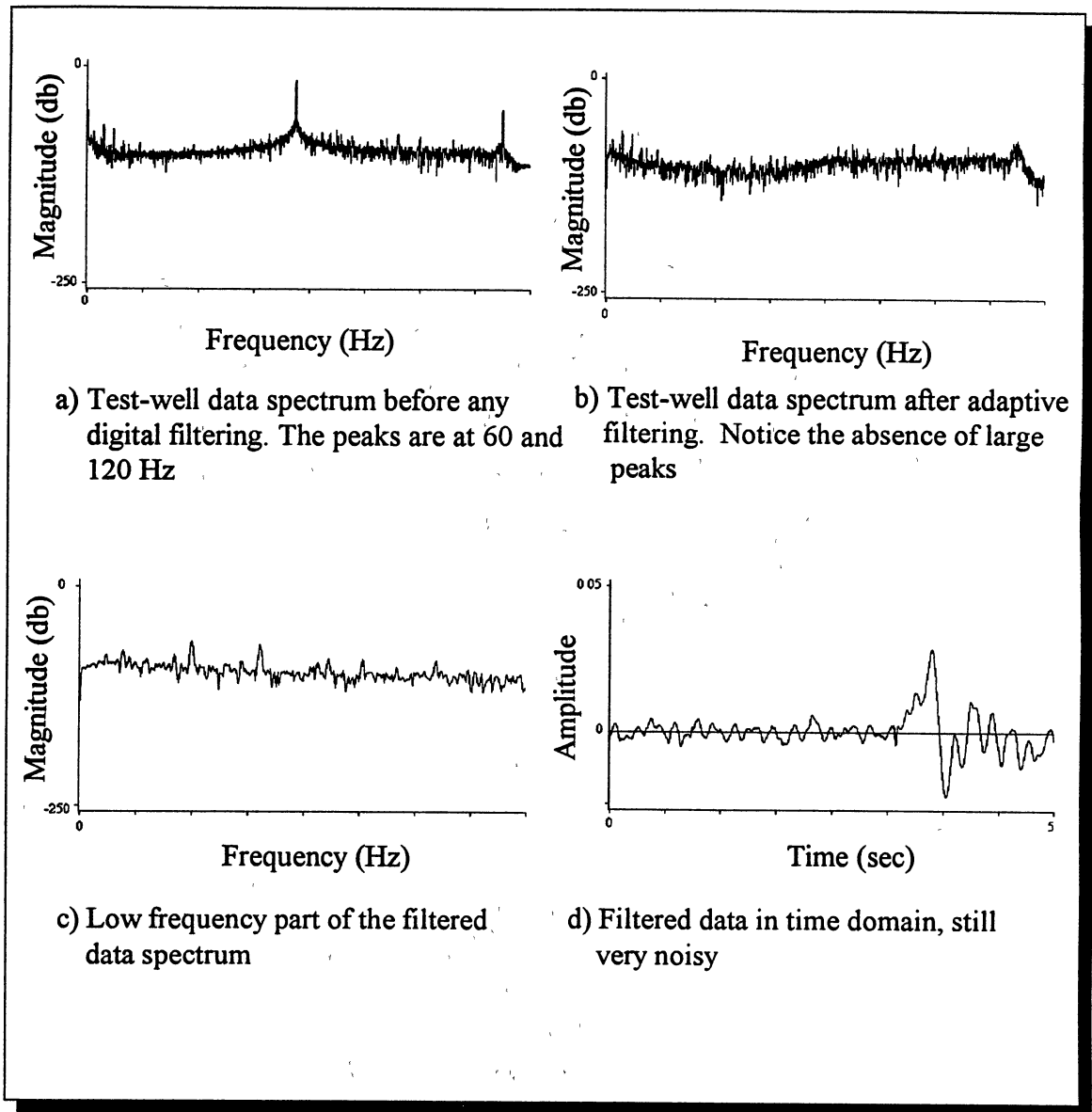
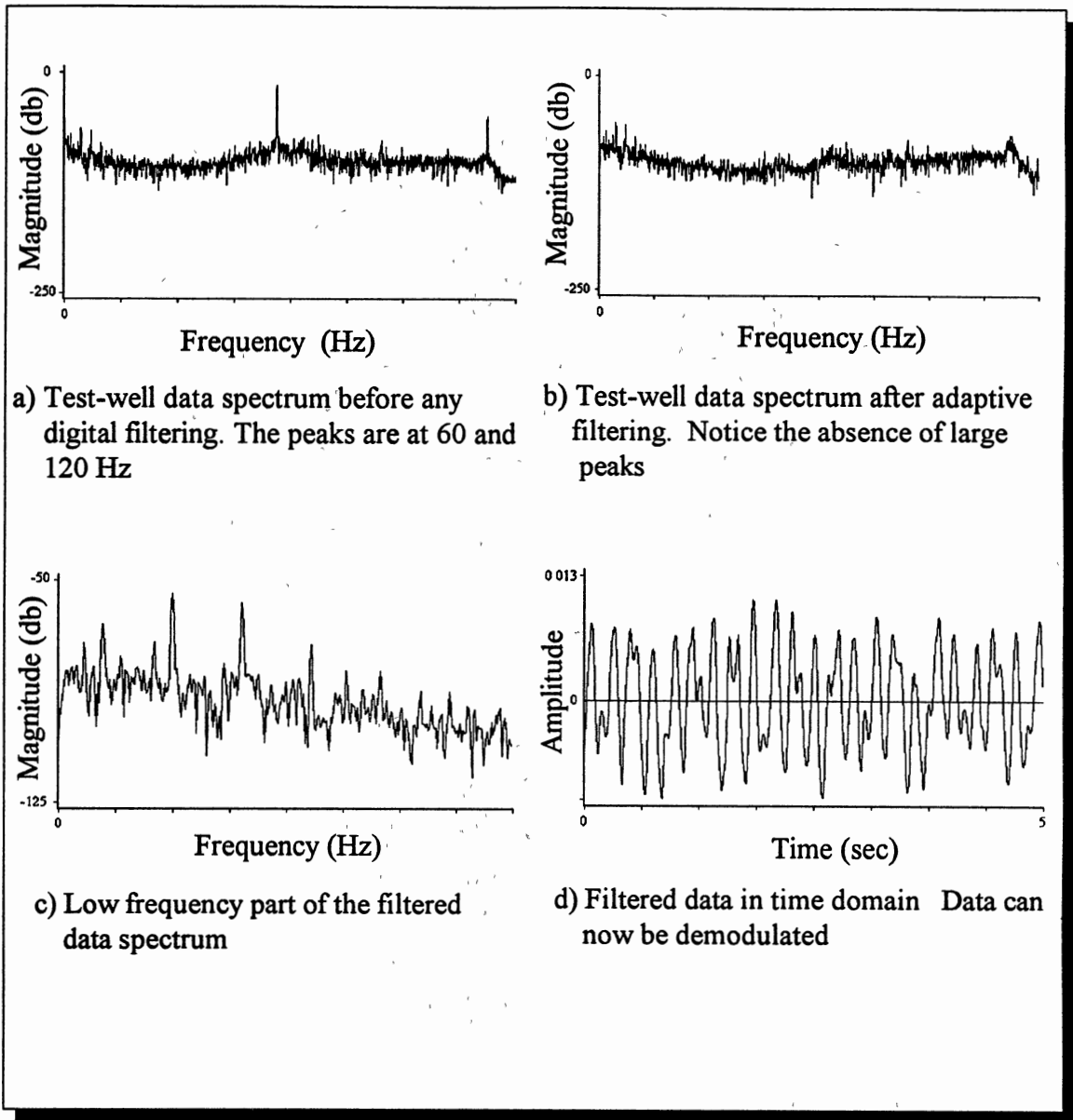


Figure 2.1- Test well data with transmitter at 3000 feet. 3Hz, 3 baud modulated signal transmitted, on a stormy day with thunder storms and rain



a) Test-well data spectrum before any digital filtering. The peaks are at 60 and 120 Hz

b) Test-well data spectrum after adaptive filtering. Notice the absence of large peaks

c) Low frequency part of the filtered data spectrum

d) Filtered data in time domain Data can now be demodulated

Figure 2.2- Test well data with transmitter at 2500 feet. 6Hz, 3 baud modulated signal transmitted on a relatively calm day

Noise Cancellation Using Adaptive Filters

The common method for estimating a signal corrupted by additive noise is to pass the corrupted signal through filters designed to attenuate the noise while changing the signal as little as possible. The filter can either be fixed or adaptive. The design of fixed filters requires some prior knowledge about both the noise and the signal. Design of adaptive filters requires little or no prior knowledge of either the signal or noise characteristics. Noise cancelling uses an auxiliary or reference input derived from sensors in the noise field where the signal is weak or nonexistent. In cases where adaptive noise cancelling is applicable, a high degree of noise cancelling is possible, so much that it may be difficult or impossible to attain by classical methods.

Some of the earliest work on adaptive interference cancelling was performed by Howell and Applebaum and their colleagues at the General Electric Company during late 1950s. Their application consisted of antenna sidelobe cancelling by using a reference antenna and a two weight adaptive filter. In 1959, Widrow and Hoff at Stanford University were working on the Least Mean Square (LMS) adaptive algorithm. In the 1960s, interest in adaptive systems grew rapidly and many papers were published on the subject. Since the 1960s many applications using adaptive algorithms have been developed. Applications such as echo cancellation on phone lines, elimination of periodic interference in general and, more recently, noise cancelling in automobiles.

An Adaptive Noise Canceller (ANC) is able to adjust its own parameters automatically as noise conditions change [10]. The canceller requires two inputs, primary and secondary. The primary input contains both signal and noise and the secondary input

contains only noise, which is correlated with the noise in the primary input. Widrow and Stearns [1], have shown that small amounts of signal present in the reference input, although undesirable, will not deteriorate the performance of the noise canceller. Noise reduction is accomplished by properly filtering the reference signal and then subtracting it from the primary signal.

The filtering of the reference signal is done using an adaptive filter. A Least Mean Square (LMS) gradient search algorithm is used to minimize an error signal [10]. The error signal is the result of subtraction of the primary signal and the output of the adaptive filter, as shown in Figure 2.3.

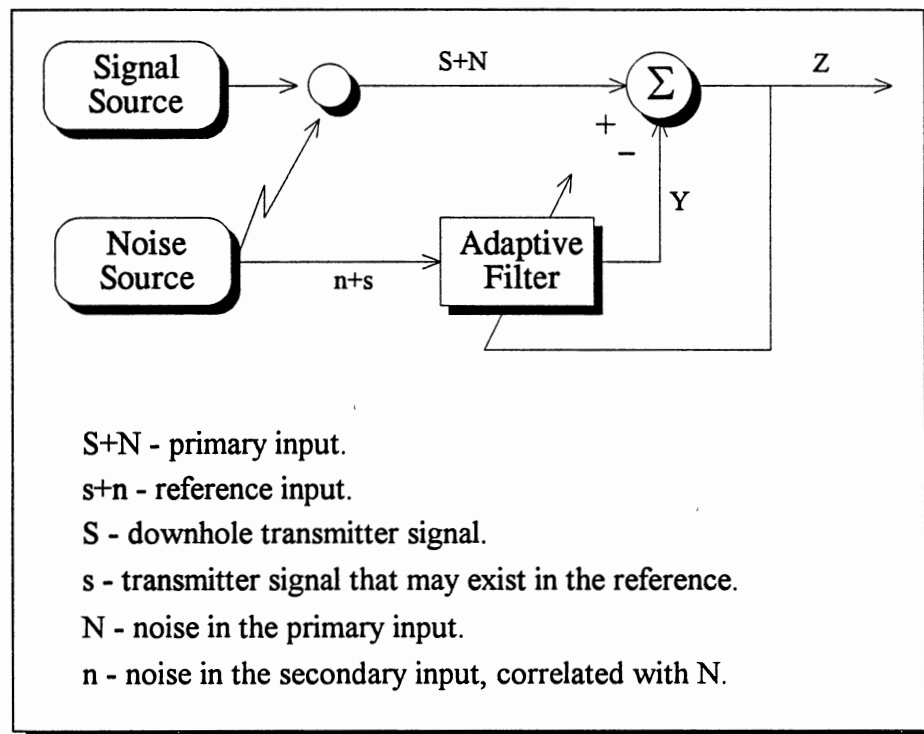


Figure 2.3- Noise cancellation

The reference input to the noise canceller should contain noise which is correlated with the primary input noise and contains as low a signal component as possible. This type of reference is available in the EBT application as is shown later in Figure 4.1. The noise cancelling algorithm minimizes the total output power which will actually minimize the output noise power.

The following shows the functionality of the adaptive noise canceller. The output of the noise canceller is $Z = S + N - Y$ as shown in Figure 2.3. S is uncorrelated with N and Y . To minimize the error, $N - Y$ needs to be minimized, which ideally leads to $Z = Y$. The minimization procedure is as follows

$$Z^2 = S^2 + (N - Y)^2 + 2S(N - Y) \quad (2.1)$$

taking the expected value,

$$\begin{aligned} E\{Z^2\} &= E\{S^2\} + E\{(N - Y)^2\} + 2E\{S(N - Y)\} \\ &= E\{S^2\} + E\{(N - Y)^2\}, \end{aligned} \quad (2.2)$$

since S is uncorrelated with N and Y .

Then

$$\min(E\{Z^2\}) = E\{S^2\} + \min(E\{(N - Y)^2\}) \quad (2.3)$$

since the signal power is unaffected by the minimization. Also since $Z = S + N - Y$ or $Z - S = N - Y$, minimizing $E\{(N - Y)^2\}$ results in an output Z that is a best least squares estimate of the signal S . If the noise in the reference signal is not correlated with the noise in the primary, then the adaptive canceller will shut itself off and will not introduce any noise to the primary signal. If Y and N are uncorrelated,

$$\begin{aligned} \min(E\{Z^2\}) &= E\{S^2\} + \min(E\{(N - Y)^2\}) \\ &= E\{S^2\} + \min(E\{N^2\} - E\{2NY\} + E\{Y^2\}) \\ &= E\{S^2\} + \min(E\{N^2\} + E\{Y^2\}). \end{aligned} \quad (2.4)$$

The minimum value is obtained when $E\{Y^2\}$ is zero. That is achieved when all the weights are set to zero.

The basic element of the noise canceller is the LMS adaptive filter [10], Figure 2.4. Its operation is described below:

Let $X_j = [x_{1j}, x_{2j}, \dots, x_{nj}]$ and $W = [w_1, w_2, \dots, w_n]$,

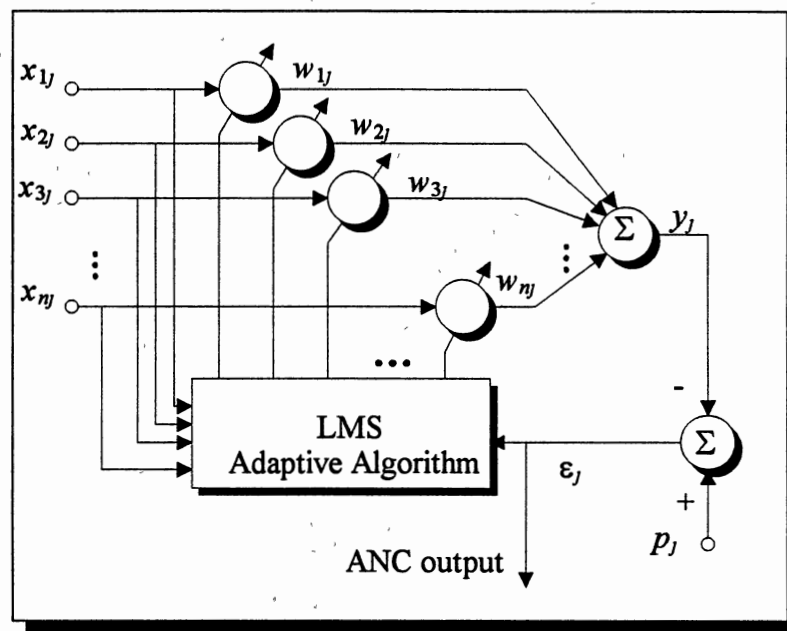


Figure 2.4- ANC

The output becomes:

$$y_j = X_j^t W = W^t X_j. \quad (2.5)$$

The error ϵ_j for the noise canceller is described as the difference between the primary input, which contains noise and signal and the filtered reference input, y_j ,

$$\epsilon_j = p_j - y_j \quad (2.6)$$

where p_j is the primary input to the noise canceller

Then

$$\epsilon_j^2 = (p_j - y_j)^2 \quad \text{or} \quad \epsilon_j^2 = p_j^2 - 2p_j X_j^T W + W^T X_j X_j^T W \quad (2.7)$$

taking the expected value,

$$E\{\epsilon_j^2\} = E\{p_j^2\} - 2E\{p_j X_j^T\} W + W^T E\{X_j X_j^T\} W \quad (2.8)$$

The cross correlation of p_j and X_j is

$$CC = E\{p_j X_j\} = E\{(p_j x_{1j}, p_j x_{2j}, \dots, p_j x_{nj})^T\} \quad (2.9)$$

The input correlation matrix is

$$R = E\{X_j X_j^T\} \quad (2.10)$$

R is symmetric, positive definite. The mean squared error will be

$$E\{\epsilon_j^2\} = E\{p_j^2\} - 2CC^T W + W^T R W \quad (2.11)$$

The LMS algorithm is used to minimize the error.

Taking the gradient of the error function,

$$\nabla E\{\epsilon_j^2\} = \left(\frac{\partial E\{\epsilon_j^2\}}{\partial w_1}, \dots, \frac{\partial E\{\epsilon_j^2\}}{\partial w_n} \right)^T \quad (2.12)$$

$$\text{or} \quad \nabla E\{\epsilon_j^2\} = -2CC + 2RW \quad (2.13)$$

Setting the gradient to zero and solving the equation, results in the optimum weight vector, W^* ,

$$W^* = R^{-1}CC \quad (2.14)$$

which is the matrix form of the Wiener-Hopf equation [4],[5]

The LMS algorithm can be used to find an approximate solution for the above in real time. There will be no matrix inversions or correlation calculations, which makes the algorithm ideal for real time applications. The LMS algorithm is an implementation of the steepest descent method where the next weight vector is calculated as:

$$W_{j+1} = W_j - \mu(\nabla_j)$$

where ∇_j is the true gradient at the j th iteration.

μ determines stability and the rate of convergence. Estimating and simplifying the gradient results in the Widrow-Hoff LMS algorithm [46]:

$$W_{j+1} = W_j + 2\mu\varepsilon_j X_j \quad (2.15)$$

Where μ is the convergence factor.

It is assumed that ε_j^2 , the square of a single error sample, is an estimate of the mean square error and so

$$\hat{\nabla}_j = \left(\frac{\partial \varepsilon_j^2}{\partial w_1}, \dots, \frac{\partial \varepsilon_j^2}{\partial w_n} \right)^t \quad (2.16)$$

$$\hat{\nabla}_j = -2\varepsilon_j X_j \quad (2.17)$$

since

$$\varepsilon_j = p_j - W^t X_j \text{ and } \frac{\partial \varepsilon_j}{\partial w_n} = -x_n$$

Starting with some initial weight vector, the algorithm will converge as long as μ is between 0 and $\frac{1}{\lambda_{\max}}$. λ_{\max} is the maximum eigenvalue of R , the input correlation matrix.

Simulation results along with actual filtered well data are shown in Figures 2.5 and 2.6. Figure 2.5a shows a plot of a 3Hz simulated sine wave and Figure 2.5b shows the same signal with added noise of much larger amplitude. The added noise is a simulated 60Hz sine wave. The inputs to the adaptive noise canceller is the data shown in Figure 2.5b and a 60Hz sine wave with a smaller amplitude and an arbitrary phase shift relative to the added noise. The result of the filter is shown in Figure 2.5c. The convergence rate was relatively slow due to a small μ . A small value for μ was chosen for presentation purposes.

Figure 2.6a shows the primary input data from a test well and 2.6b shows the reference, which is the data collected from the reference antenna. The desired signal is a binary phase shift keyed (PSK) 6Hz carrier. As can be seen in Figure 2.6c, the adaptive noise canceller is very effective in removal of the noise. Figure 2.6d shows the output signal when it has been passed through a second order digital Butterworth filter.

In order to remove any dc bias introduced to the data by the A/D process, a bias weight can be added to the noise canceller. Any of the weights can be used as the bias weight by setting the corresponding to a constant value, usually 1. However, since this extra weight will also remove slowly varying drifts in the data, it will reduce the SNR by attenuating the signals of interest which are in fact slow varying wave forms. Another more helpful remedy is to use a second ANC stage with only a few weights and with its reference input set to a constant value. The ANC will act as a high pass filter and will remove the dc component without any significant reduction in the signal-to-noise ratio. A graphical comparison of the performance of the two methods is shown in Figure 2.7.

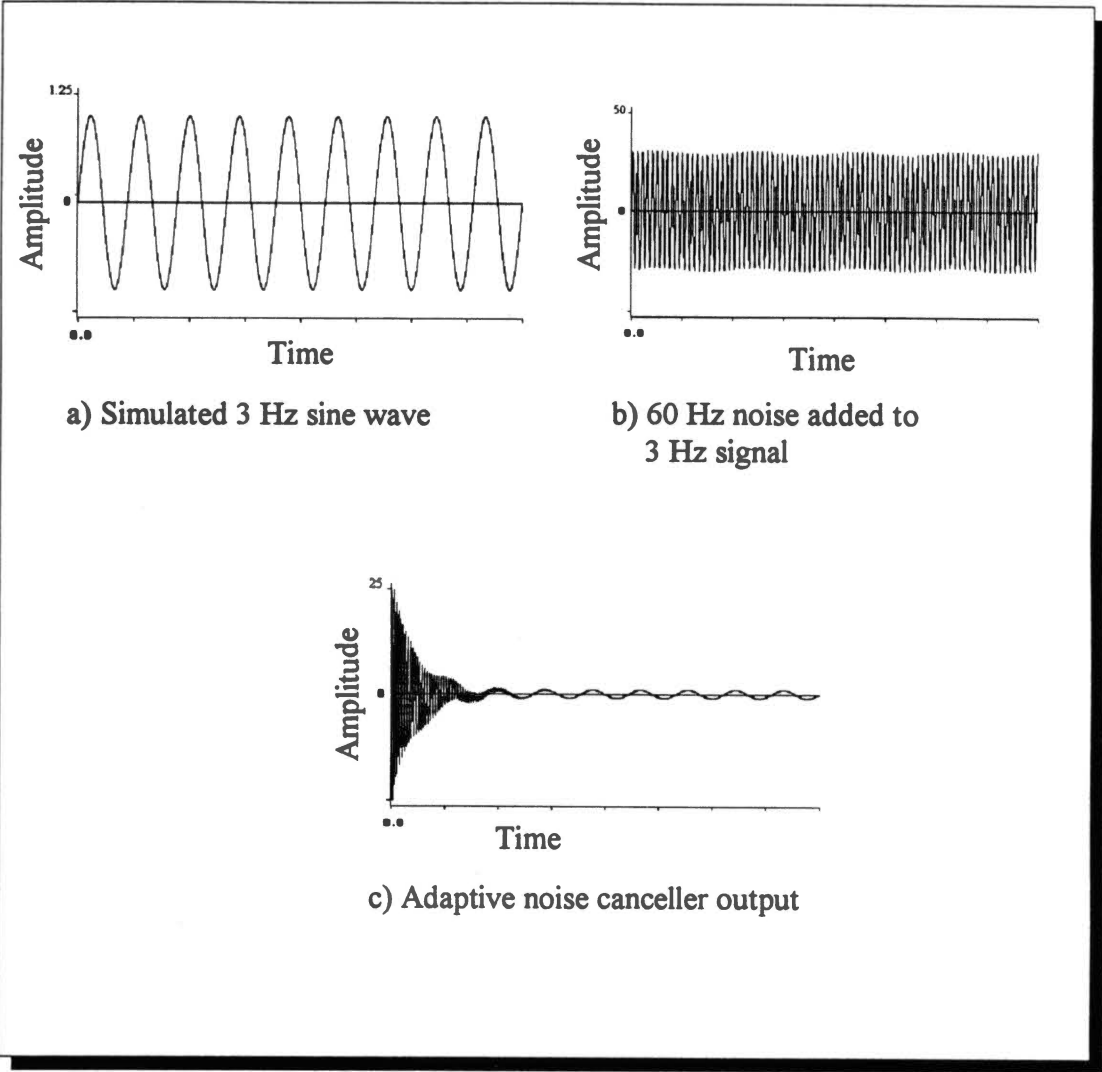


Figure 2.5- Adaptive noise canceller simulation results

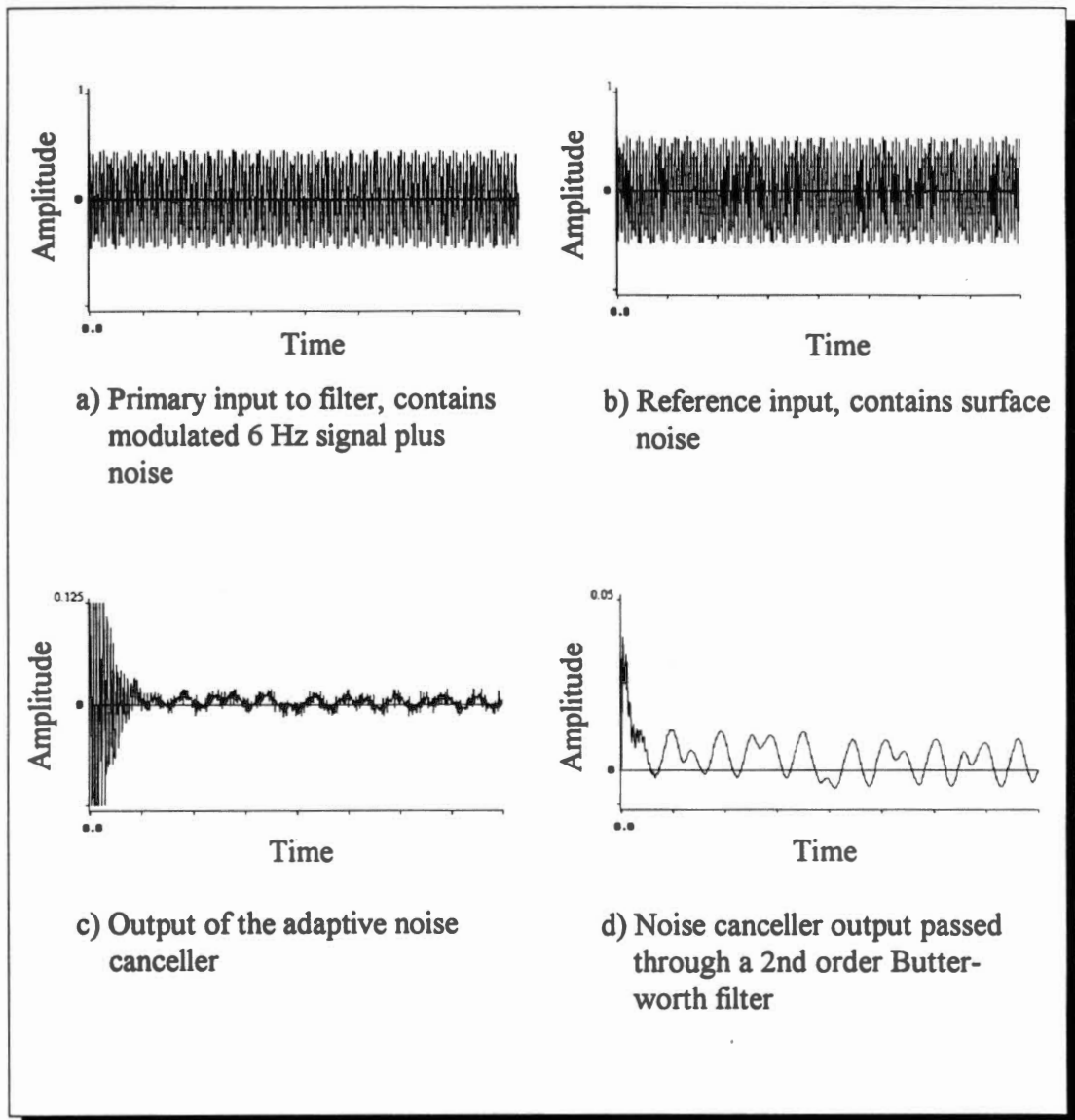


Figure 2.6- Filtering PSK 6 Hz signal using adaptive noise canceller.

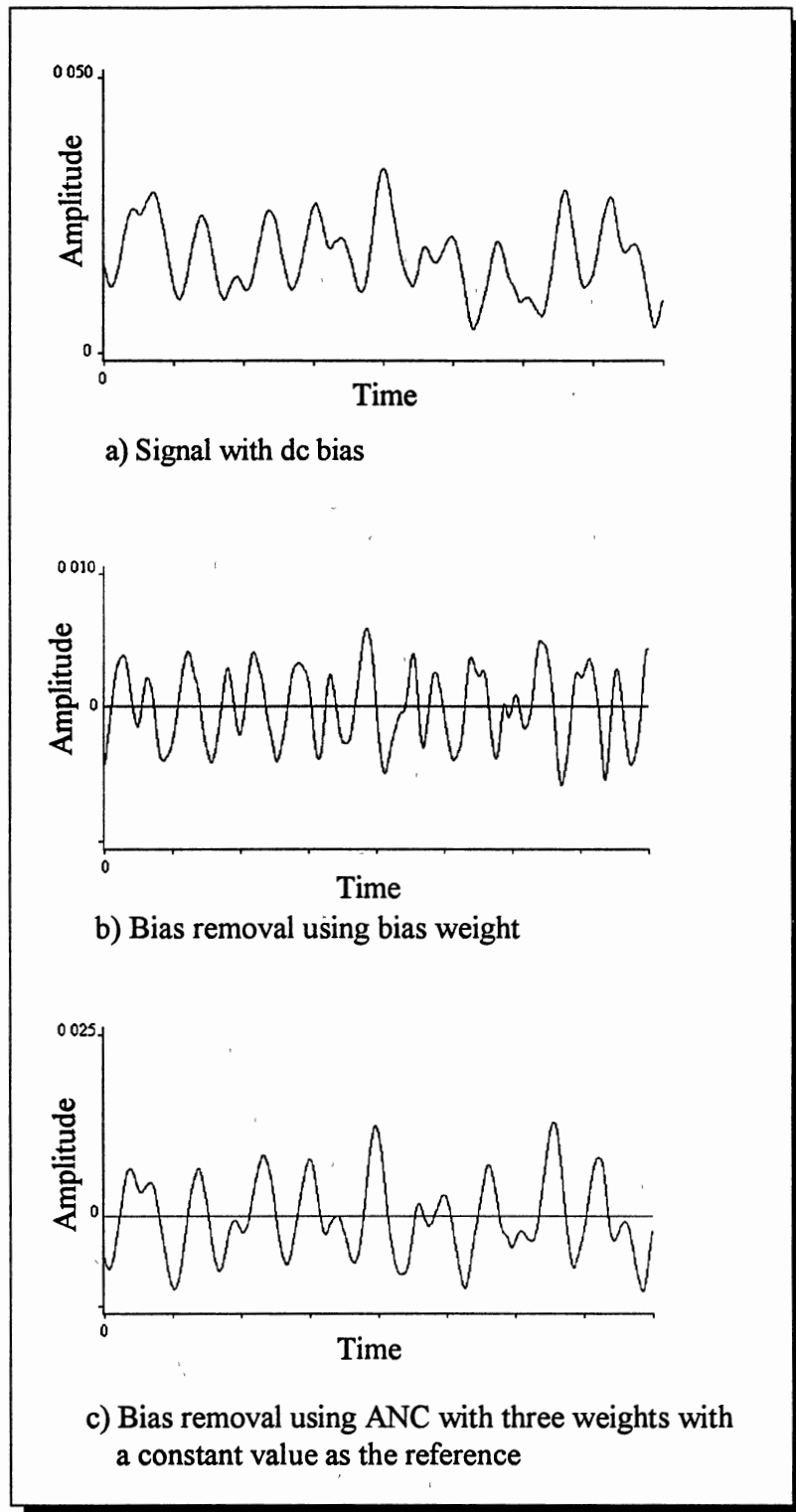


Figure 2.7- Bias removal

Impulsive noise removal for low sample rate data

The processing method for the EBT signals requires that as little impulsive noise be present in the sampled data as possible. The sampled data is passed through an LMS adaptive filter stage for removal of unwanted periodic disturbances. Adaptive filters are not well behaved in the presence of impulsive noise, hence the requirement for an impulse removal filter.

The signals of interest in the EBT communications system are in the Extremely Low Frequency (ELF) range of the spectrum. For proper processing, long intervals of data are needed for analysis. To limit the number of data points digitized in any time interval in order to reduce computation time and allow for real time operations, the sampling rate of the A/D system must be limited

Conventional signal processing techniques assume that the signal degradation is a known, time invariant quantity. They operate in an open-loop fashion where no feedback is used. For most geophysical data processing such as EBT, the amount and type of noise vary with time and location. This is due to varying surface conditions and the lithology of areas of operations. A suitable filtering technique for such operations is one which adjusts its own parameters as conditions change. This type of filter is called an adaptive filter. Adaptive processors operate in a closed-loop fashion. The input signal is filtered and then compared against a desired, conditioning or a training signal. The comparison yields an error measure $\epsilon(n)$. This error is then used to adjust the filter parameters so that the error is progressively minimized. For most real time operations the Least Mean Square (LMS)

gradient search is used to minimize the error because of its simplicity and fast settling time.

The primary input to the EBT signal processor is the signal received from the well by the antennas connected to the well head. The primary input contains the desired EBT signals plus all the noise that is to be filtered out. The secondary input is used as a reference for the adaptive filter to be subtracted from the primary. The reference antenna is not connected to the well head and contains only the surface noise.

The best performance with LMS adaptive filters is achieved when as much of the data as possible is present. In other words, one should keep as much of the signal undisturbed as possible for both inputs. This will ensure proper cancellation of the unwanted noise.

To achieve the best results from the filter and to be able to perform the EBT signal analysis in real time, the number of points in a block of data was limited to 4096. The sampling rate was set at 512 Hz with the anti-aliasing filter frequency set at 200 Hz. These settings provide the system with enough information to process the data with acceptable accuracy in real time. The highest frequency noise components of significant amplitude are 60 Hz and its harmonic at 120 Hz. The 512 Hz sampling rate is not much greater than the Nyquist¹ rate for the data. This relatively low sampling rate causes problems for impulse removal filters as described below. A new filtering method is proposed that performs without the problems associated with the other methods.

When impulsive noise is present in digital data, median filters are often used as a remedy. Median filters run a sliding window over the data and at each step filter the data

¹ The Nyquist sampling rate is defined as twice the frequency of the maximum frequency content of the data.

by replacing the point in the middle of the window by the median of the points inside the window. For example, if one uses a three point window and the values inside are 12, 5 and 30, the value 5 is replaced by 12, which is the median value of the three points. A window of length $2N+1$ can remove impulsive noise of width N . For high sample rate² data, the median filter works well without introducing much distortion to data. For low sample rate cases, the median filter can introduce significant unwanted distortion. Assume a 60 Hz signal with a sampling rate not much greater than the Nyquist rate, say 256 Hz. This results in 4 samples per cycle of the 60 Hz signal, see Figure 2.8. Running a median filter with a window width of 3 on this data to remove one point impulsive noise will distort the signal as shown in Figure 2.9. The distortion is largely due to the small number of samples present per cycle of the sine wave. For any given change in time, Δt , the change in magnitude, Δx , is large. The peak points look like spikes to the median filter and are flattened. This type of distortion is highly undesired when one considers the large error values relative to the very small signals of interest that can be over 60 db below the noise amplitude.

Another possible filtering method with smaller total error is one in which the data is scanned and only changed if impulses are detected. The impulse data are replaced by a piecewise-linear estimated value calculated using two previous data points. Even though this method reduces the total error, it still does not result in acceptable estimates for the noisy data points. Figure 2.10 shows a series of plots which explains why the results of the linear estimate method are not acceptable.

² High sample rate relative to the Nyquist rate.

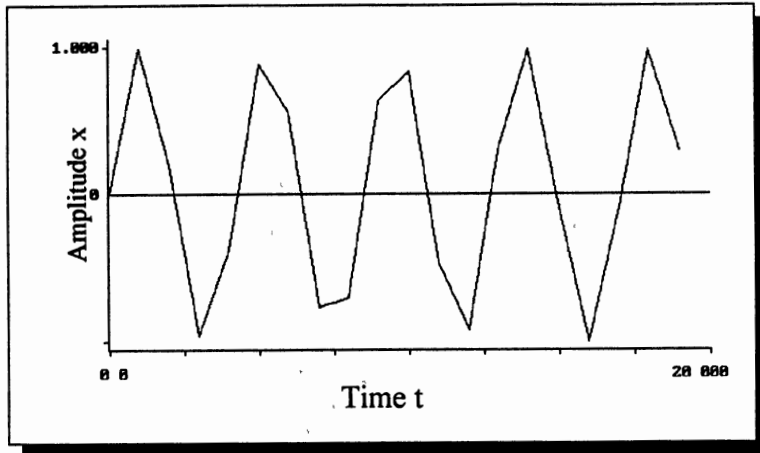


Figure 2.8- 60 Hz sine wave sampled at 256 Hz

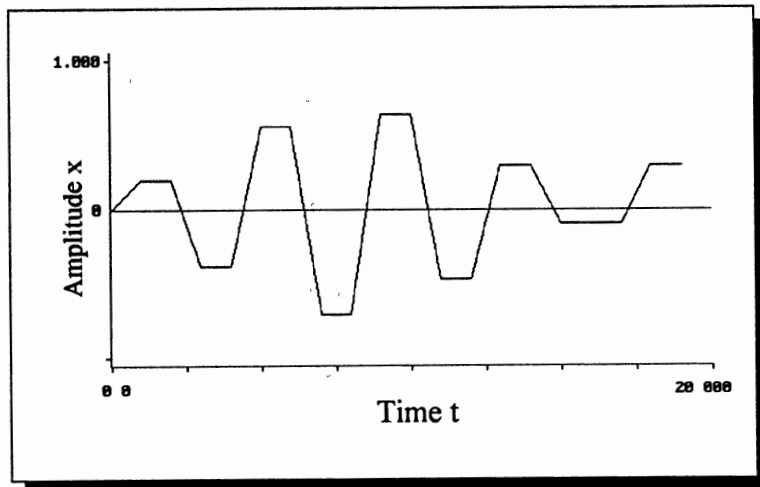


Figure 2.9- Median filter result

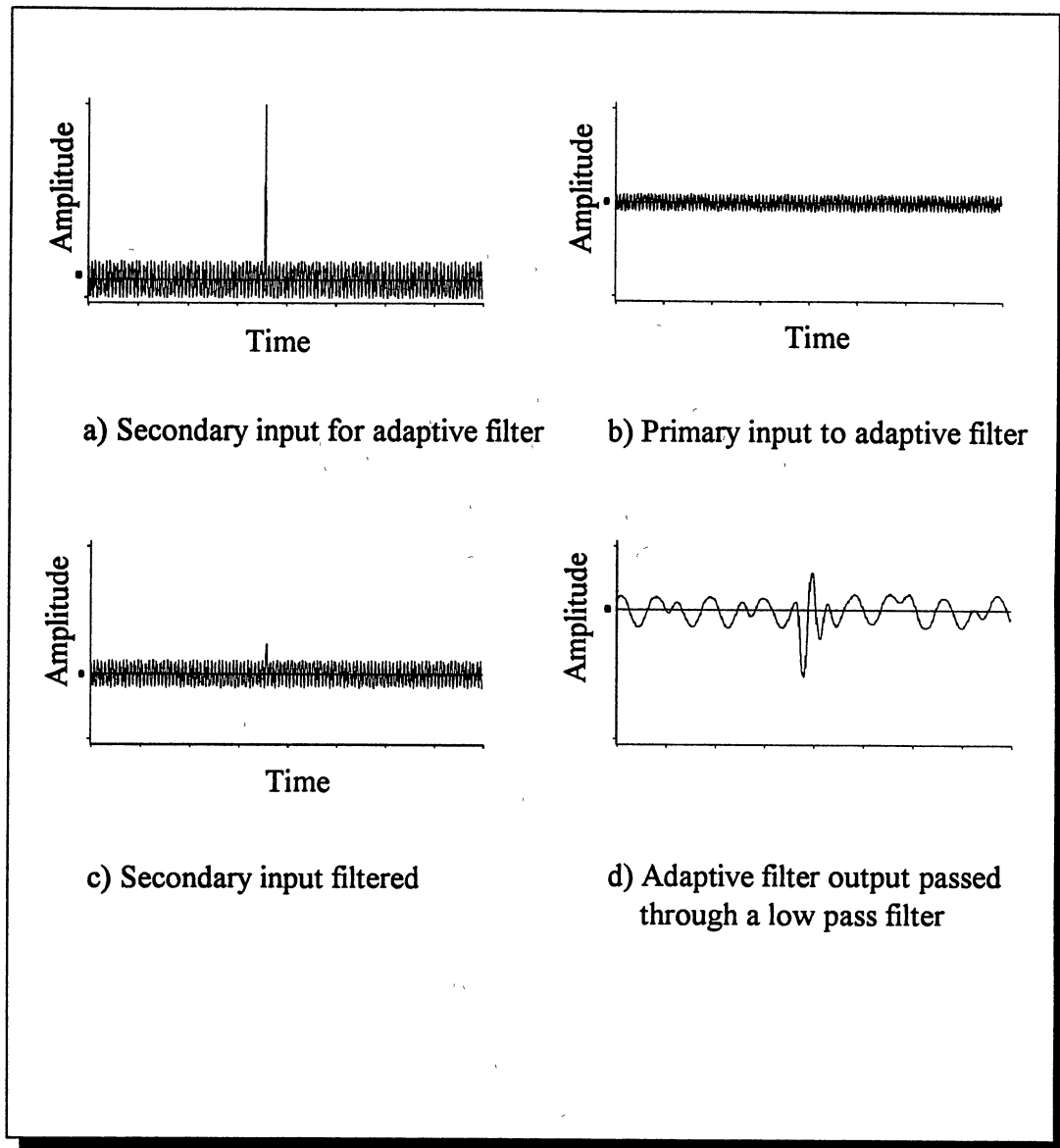


Figure 2.10- Using linear estimation method on EBT signals,
The effect of the spike can be seen in d

Figure 2.10a is a plot of the secondary input data for the adaptive filter and Figure 2.10b shows a plot of the primary input. The data plotted is actual EBT data collected from a test well. The output of the filter is shown in Figure 2.10c, where the spike has been replaced by a new value of a much smaller magnitude. Figure 2.10d is the output of the LMS adaptive filter after being passed through a low pass filter. The effect of the impulse noise can be seen in the middle part of the graph where ringing has occurred. The signal in Figure 3d has an amplitude approximately 30 db below the input signal. Errors that are small relative to the input signal are large relative to the EBT signals.

An ideal filter for impulsive noise removal is one that removes only the impulses and that will not distort any other data points. After the impulses have been removed, they must be replaced by suitable values. Different types of estimators can be used for this purpose. For example, the new value may be set to the previous value, the median or a piece-wise linear estimate. These methods may be useful for high sample rate data; however, for low sample rates, other methods that minimize the estimation error are needed. The method proposed here requires relatively longer computation time but reduces the total error considerably

The spectrum of an impulse is a constant value. If this value is determined and subtracted from the data spectrum, the result would be the data set without the impulses. Sample data sets can be used to gain information about the nature of the impulsive noise present and to estimate a threshold value in the frequency domain for impulse cancellation. The impulses are removed by zeroing out the frequency components that fall below the threshold.

If the input data is represented by $x(n)$, and the output of the filter is represented by $y(n)$, then the spectrum or Fourier transform of input data is calculated to be

$$X(k) = \sum_{n=0}^{N-1} x(n) \cdot e^{-j\frac{2\pi k n}{N}},$$

where N is the number of data points.

The output spectrum is

$$Y(k) = X(k) \cdot \Phi(|X(k)| - \alpha), \quad (2.18)$$

where α is the frequency threshold and $\Phi()$ is the unit step function

Then the filter output is given by the inverse Fourier transform of $Y(k)$

$$y(n) = \frac{1}{N} \sum_{k=0}^{N-1} Y(k) \cdot e^{j\frac{2\pi k n}{N}}$$

Figures 2.11a through 2.11d show this procedure. The data plotted is EBT data collected with added simulated impulsive noise

One may reach the conclusion that at this point the desired results have been achieved. This would be the case if none of the desired signal frequency components falls below the threshold. Otherwise, not only the impulses are removed, but some useful data has also been lost. In cases such as the EBT, where the desired signal amplitudes are very small compared to the noise, more needs to be done to reduce the total error. Setting the above filtered data as a reference to an adaptive clipping stage will reduce the total error considerably. In the clipping stage, the non-filtered data is scanned and as spikes are detected, they are replaced by the corresponding value in the reference. This way only the spikes are changed and the total error is reduced. The spikes are detected by numerically differentiating the data and searching for maxima. The maxima are then compared to a maximum allowable slope. If any of them is greater than the maximum slope, they are considered to be spikes. The following are the operations performed by the filter:

1. Frequency domain filtering.
 - a- Calculate FFT of the signal.
 - b- Zero out the frequency components which fall below the threshold.
 - c- Calculate IFFT.
2. Detect the impulses in the data set, then replace them with corresponding output data of step 1.

The crucial parts of this procedure lie in determination of the frequency domain filter threshold for step 1 and the maximum slope for step 2. The latter is determined as a multiple of the root mean square (rms) value of the data set divided by the sampling period, Δt . The latter is determined by inspection of the data spectrum. Excellent results were obtained using a threshold just above the noise floor in the data spectrum (Figure 2.11b) and twice the rms value of the data for maximum slope.

Figure 2.12 shows a block diagram of the filtering procedure. The third block, Fftfil, is where the frequency domain filtering takes place and the last block, Clipper, replaces the impulses with proper values. Figure 2.13 shows a graphical comparison of the three filtering methods described here. A commonly used quantitative comparison of the performance of digital filters is the empirical mean square error given by

$$\varepsilon = \frac{1}{K} \sum_{i=1}^K (f_i - x_i)^2 \quad , \quad (2.19)$$

where K is the number of samples, x_i is the original data without impulsive noise, and f_i is the filtered data. The smaller the error, the better the performance of the filter. The ideal case is when f_i matches x_i exactly, which reduces the error, ε , to 0. Calculating ε for the 256 point data set of Figure 2.13 results in:

$$\begin{aligned}\epsilon_{\text{median}} &= 3.18 \times 10^{-2} \\ \epsilon_{\text{linear}} &= 1.78 \times 10^{-3} \\ \epsilon_{\text{filt}} &= 4.64 \times 10^{-6}\end{aligned}$$

The smallest mean square error is that of ϵ_{filt} , the proposed filter.

In conclusion, it can be said that the proposed method of impulse removal produces better results than other impulse filtering methods in terms of error minimization on this type of data. The drawback is the longer computation time which may prove too long for some applications, especially when real time processing is concerned. In applications such as the EBT system, where the data sample rate is slow, the processor is provided with ample time to analyze the data. This method is also useful for non-real time applications where the data is collected and recorded prior to any processing

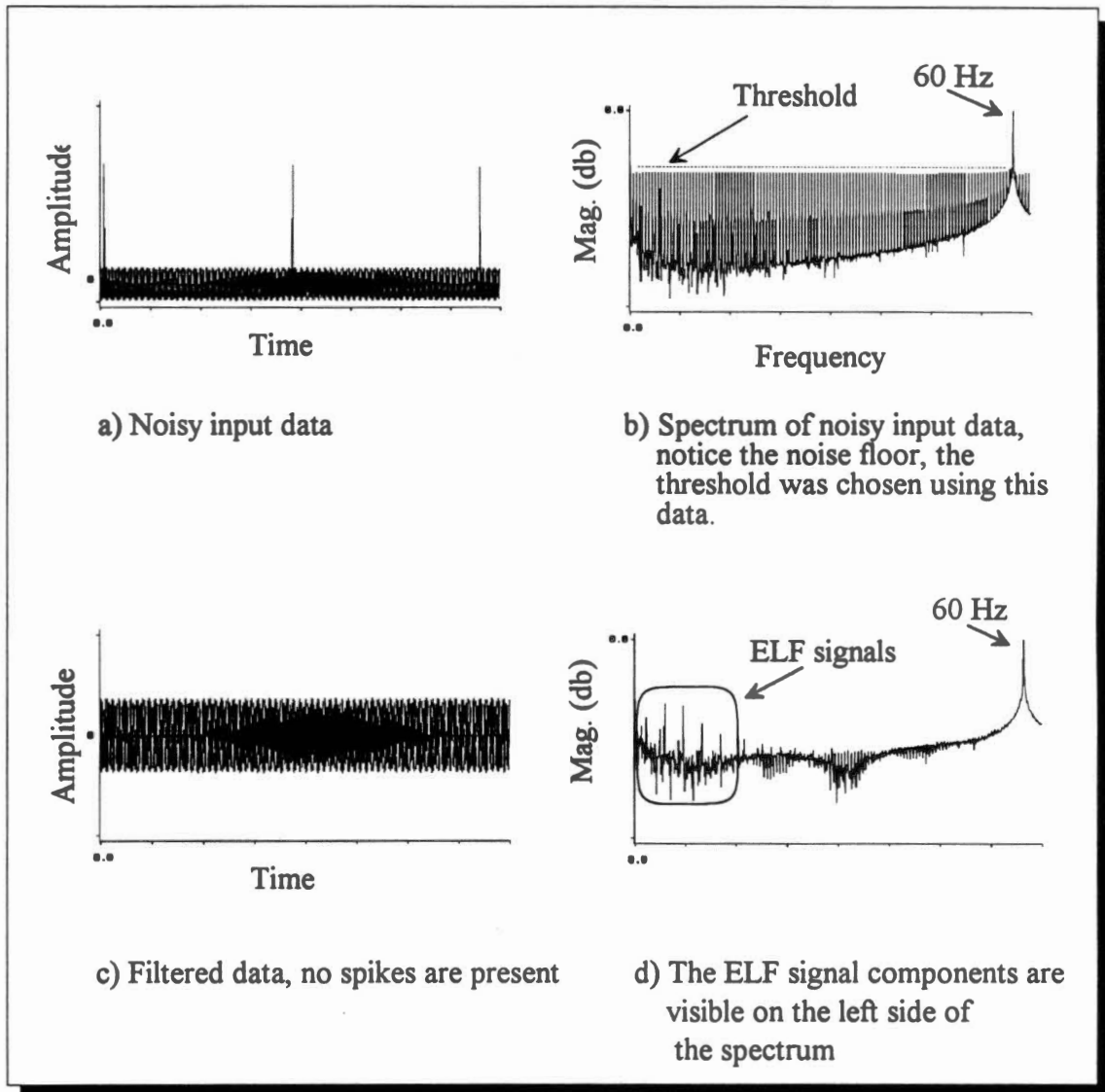


Figure 2.11- Impulsive noise removal using the proposed method

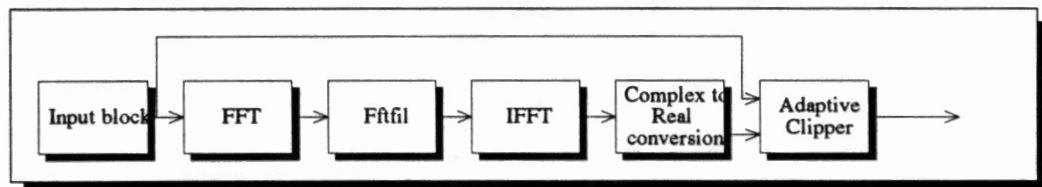


Figure 2.12- The block diagram of the proposed filter

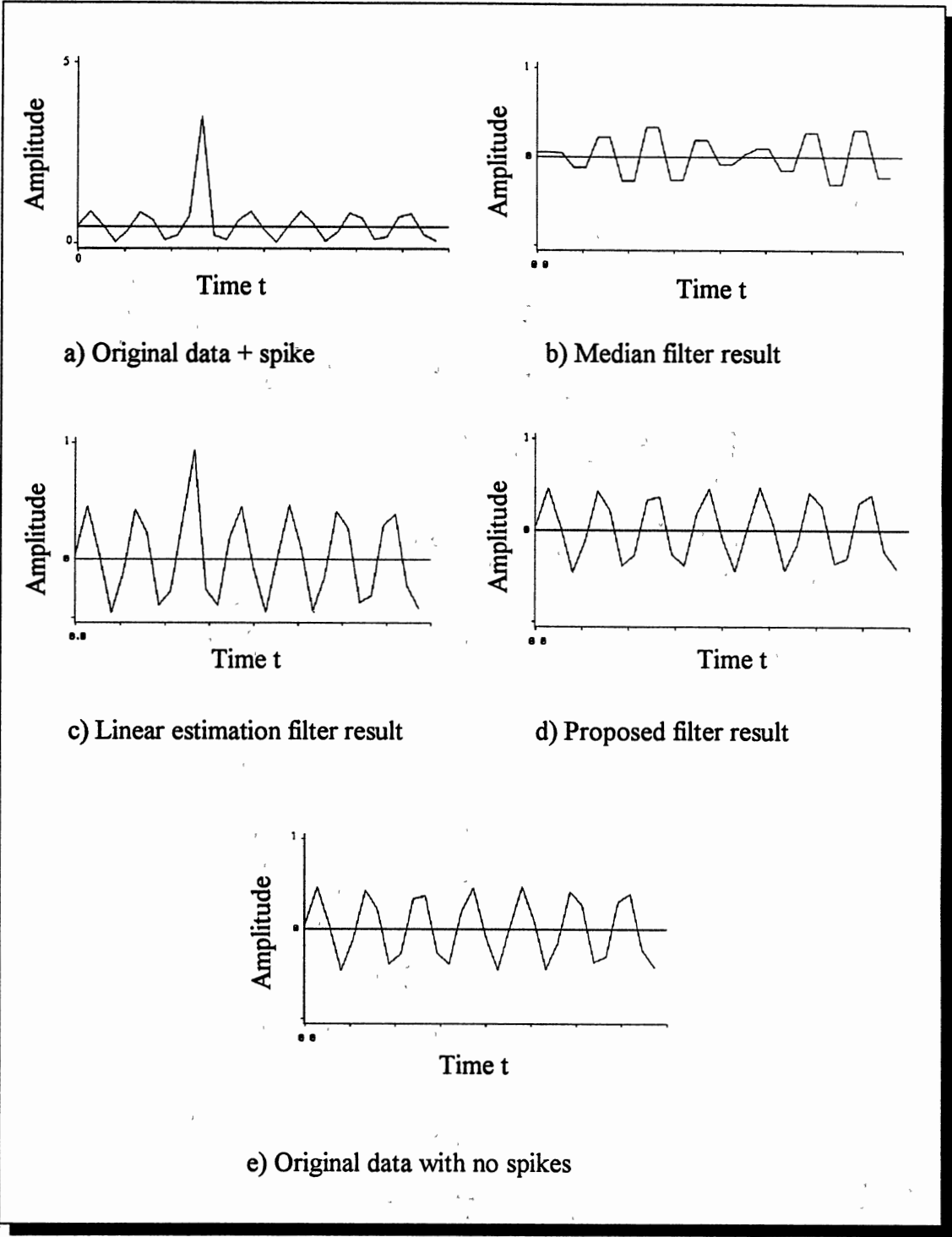


Figure 2.13- A comparison of different filtering methods

CHAPTER III

DIFFERENTIAL PHASE SHIFT KEYED (DPSK)

MODULATION/DEMODULATION

A bi-phase modulation scheme was chosen for transmission of data through the earth as it is the modulation/demodulation method with the lowest probability of error as compared to other methods [2]. The optimal demodulator for such a modulation system is the correlation detector if a coherent reference is available at the receiver. However, the assumption of coherence is non-trivial, implying some method of accurate time-basing between transmitter and receiver, e.g., a phase-locked loop. Due to the fading characteristic of the channel, the earth, it is difficult to obtain a coherent reference. A noncoherent demodulation method would be the method of choice in situations where the channel is of a fading type and signal attenuation rate changes randomly.

The salient point is the acquisition and tracking of the phase of the received signal. One way of accomplishing this phase tracking is to use the carrier phase of the immediately preceding signal interval as the phase reference for the current interval. Two conditions are necessary for such a scheme to be effective. First, the phenomenon that causes the unknown phase drift in the transmitted signal must vary slowly enough that the phase change is negligible from one bit interval to the next. For the EBT application, this in turn implies some method of spike removal in the received signal, such as the use of

summation of multiple antennas or the use of a median filter or other nonlinear operations. These noise spikes are the only significant causes of rapid phase shifts in the current application. Other phase drift may occur, but would be so small that the condition of constant phase from bit interval to bit interval would still hold.

Second, the phase of one signaling interval must have a known relationship to the phase of the next interval. This condition can be ensured by employing differential encoding of the signal. The encoding process relates the signaling intervals by using an arbitrary binary reference digit. This method determines only the phase shifts in the transmitted signal and not the exact phase. Figure 3.1 shows an example of differential encoding of a message sequence. The reference bit in Figure 3.1 is assumed to be a binary zero, the reference is then compared to the first message bit that is a one, since there is a change, the encoded bit would be a one. The output would have been a 0 if the bit value had not changed from the previous interval. The rest of the message is encoded this way. The encoded message then modulates a carrier by shifting its phase by either 0 or π radians. A block diagram of the encoding algorithm is shown in Figure 3.2. The message sequence is passed through an equivalence stage which compares the current bit value with the previous one and then the result is passed through a level shift circuit which outputs either a "+1" or a "-1". The output of the level shifter is then used to modulate the carrier. The equivalence stage has a similar logic to that of an exclusive-nor gate. The exclusive-nor gate is shown in Figure 3.3.

Message sequence	1 0 1 1 1 0
Encoded sequence	0 1 1 0 1 0 0
	ref.
Carrier Phase	π 0 0 π 0 π π

Figure 3.1- Differential Encoding

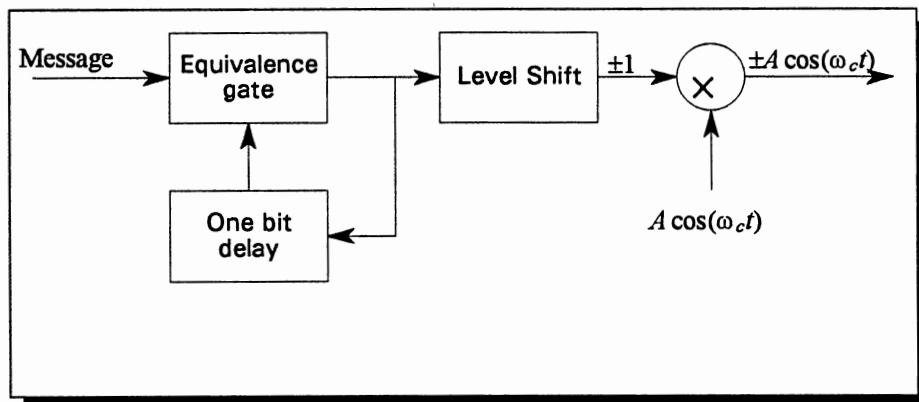


Figure 3.2- Dpsk demodulator

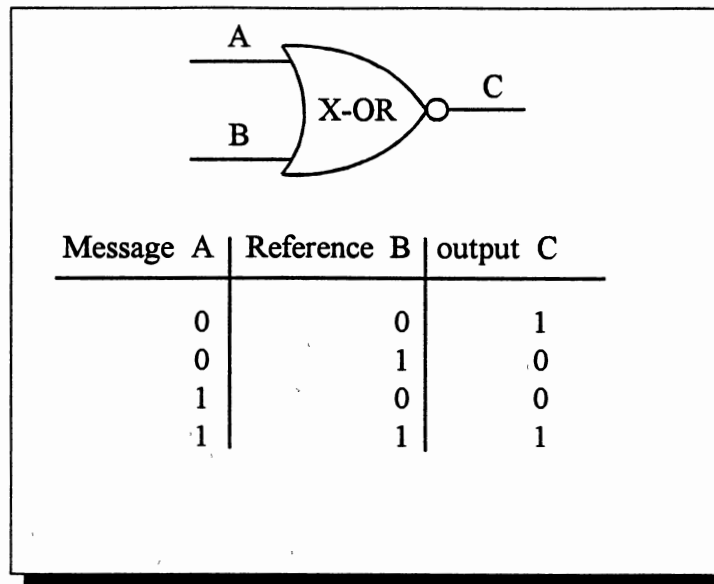


Figure 3.3- Equivalence gate

In order to maintain a coherent bit rate at the surface receiver and the downhole transmitter, the surface demodulator needs to have a reference of the carrier frequency. The reference does not need to be in phase with the downhole transmitter, it only needs to have the same frequency. In the absence of such reference, a good estimate of the carrier frequency could be used. The use of the carrier frequency estimate will prevent any data loss due to slow frequency drifts of the transmitter. To estimate the carrier frequency a squaring method is used wherein a processed block of data is squared and its Fourier transform is calculated. The spectrum of the data is then searched for the frequency at which the maximum value occurs, that frequency is twice the actual carrier frequency.

The search is performed in the neighborhood of the previous peak value. Figure 3.4 shows a block diagram of the frequency estimator.

The estimation error has a maximum magnitude of $\frac{df}{2}$ where $df = \frac{f_r}{N}$. The error is a function of the transmitter frequency and is a zero mean, uniformly distributed random variable because it is equally likely for the actual carrier frequency to fall anywhere inside a frequency interval.

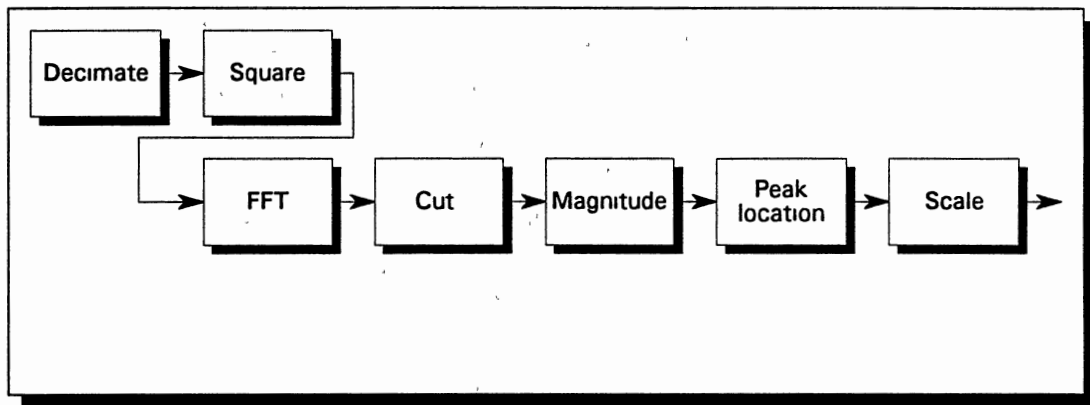


Figure 3.4- Carrier Frequency Estimation

Probability of Error for Optimal DPSK Demodulation System

Figure 3.5 shows a schematic of the demodulator.

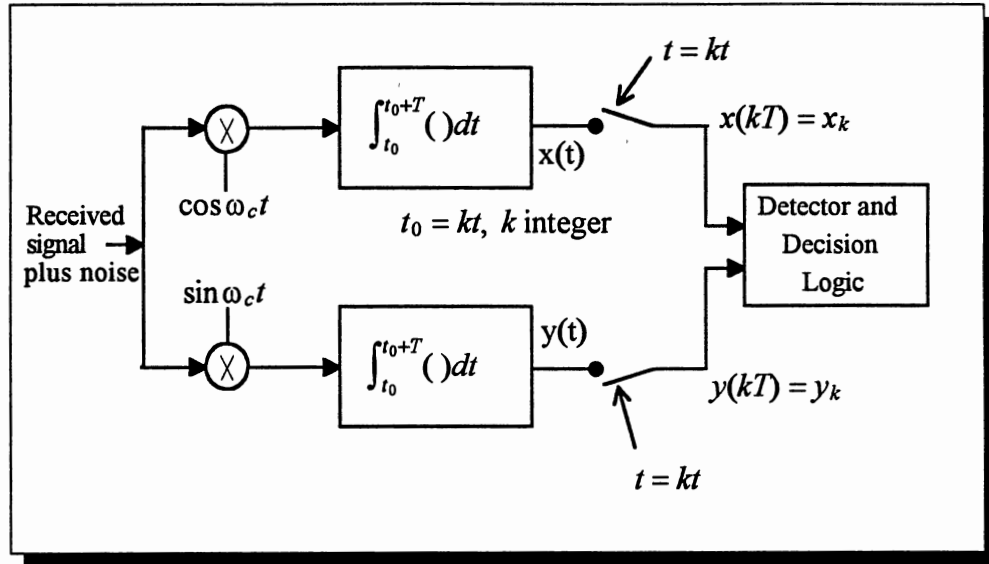


Figure 3 5- Optimum DPSK demodulator

Detector output is

$$l = x_k x_{k-1} + y_k y_{k-1} \quad (3.1)$$

$$\text{If } l > 0, \quad \text{then } S_1(t) = \begin{cases} A \cos(\omega_c t + \theta) & -T < t < 0 \\ A \cos(\omega_c t + \theta) & 0 \leq t < T \end{cases} \quad (3.2)$$

$$\text{If } l \leq 0, \quad \text{then } S_2(t) = \begin{cases} A \cos(\omega_c t + \theta) & -T < t < 0 \\ -A \cos(\omega_c t + \theta) & 0 \leq t < T \end{cases} \quad (3.3)$$

Let $\theta = 0$ with no loss of generality, then the probability of error in the receiver when S_1 is sent and S_2 is detected (or vice versa) becomes,

$$P_E = P_r(x_k x_{k-1} + y_k y_{k-1} < 0 | S_1 \text{ sent}, \theta = 0), \quad (3.4)$$

assuming that S_1 and S_2 are equally likely and that $\omega_c T$ is an integer multiple of π .

Outputs of the integrator at $t = 0$ are

$$x_0 = \frac{AT}{2} + n_1 \quad (3.5)$$

$$y_0 = n_3 \quad (3.6)$$

where

$$n_1 = \int_{-T}^0 n(t) \cos(\omega_c t) dt \quad (3.7)$$

and

$$n_3 = \int_{-T}^0 n(t) \sin(\omega_c t) dt \quad (3.8)$$

At time $t = T$,

$$x_1 = \frac{AT}{2} + n_2 \quad (3.9)$$

$$y_1 = n_4 \quad (3.10)$$

where

$$n_2 = \int_0^T n(t) \cos(\omega_c t) dt \quad (3.11)$$

and

$$n_4 = \int_0^T n(t) \sin(\omega_c t) dt \quad (3.12)$$

$n(t)$ is white Gaussian noise with double-sided power spectral density N_0/T and n_1, n_2, n_3 and n_4 are uncorrelated, zero mean Gaussian random variables with variances $\frac{N_0 T}{4}$. See Figure 26.

$$P_E = P_r\left[\left(\frac{AT}{2} + n_1\right)^2 \left(\frac{AT}{2} + n_2\right)^2 + n_3 n_4 < 0\right] \quad (3.13)$$

or

$$P_E = P_r\left[\left(\frac{AT}{2} + \frac{n_1}{2} + \frac{n_2}{2}\right)^2 - \left(\frac{n_1}{2} - \frac{n_2}{2}\right)^2 + \left(\frac{n_3}{2} + \frac{n_4}{2}\right)^2 - \left(\frac{n_3}{2} - \frac{n_4}{2}\right)^2 < 0\right] \quad (3.14)$$

Defining new Gaussian random variables as

$w_1 = \frac{n_1}{2} + \frac{n_2}{2}$, $w_2 = \frac{n_1}{2} - \frac{n_2}{2}$, $w_3 = \frac{n_3}{2} + \frac{n_4}{2}$ and $w_4 = \frac{n_3}{2} - \frac{n_4}{2}$ results in

$$P_E = P_r[(\frac{AT}{2} + w_1)^2 + w_3^2 < w_3^2 + w_4^2] \quad (3.15)$$

The new random variables are uncorrelated, independent random variables with zero mean and variance $\frac{N_0T}{4}$.

Letting $R_1 = \sqrt{(\frac{AT}{2} + w_1)^2 + w_3^2}$ and $R_2 = \sqrt{w_3^2 + w_4^2}$,

$$P_E = P_r[R_1 < R_2] \quad (3.16)$$

or
$$P_E = \int_0^\infty [\int_{r_1}^\infty f_{R_2}(r_2) dr_2] f_{R_1}(r_1) dr_1 \quad (3.17)$$

where R_1 is a Rician distributed random variable and R_2 is a Rayleigh distributed random variable with

$$f_{R_1}(r_1) = \frac{r_1}{N} e^{-\frac{A^2+r_1^2}{2N}} I_0(\frac{Ar_1}{N}), r_1 \geq 0, \text{ where } N = \frac{N_0}{T} = N_0B_T \quad (3.18)$$

$I_0 = \frac{1}{2\pi} \int_0^{2\pi} e^{v \cos u} du$ is a modified Bessel function of the first kind and zero order, and

$$f_{R_2}(r_2) = \begin{cases} \frac{r_2}{N} e^{-\frac{r_2^2}{2N}}, r_2 \geq 0 \\ 0, r_2 < 0 \end{cases} \quad (3.19)$$

To solve for P_E , the inner integral simplifies as

$$\int_{r_1}^\infty f_{R_2}(r_2) dr_2 = e^{-\frac{r_1^2}{2N}} \quad (3.20)$$

and

$$P_E = e^{-Z} \int_0^\infty \frac{r_1}{N} I_0(\frac{Ar_1}{N}) e^{-\frac{r_1^2}{2N}} dr_1, \text{ where } Z = \frac{A^2}{4N} \quad (3.21)$$

From table of integrals,

$$P_E = \frac{1}{2} e^{-Z} \quad (3.22)$$

This value can be compared to other digital binary signaling schemes. For coherent PRK signals, $P_E = \frac{1}{2\sqrt{\pi Z}} e^{-Z}$ for $Z \gg 1$. For large signal-to-noise ratios, DPSK and coherent

PRK differ by a very small amount. For coherent FSK signals, the probability of error is $P_E = \frac{1}{2} \operatorname{erfc}(\sqrt{\frac{1}{2}Z})$ where $\operatorname{erfc}(x) = \frac{2}{\sqrt{\pi}} \int_0^x e^{-t^2} dt$, which is the same as probability of error for coherent Amplitude Shift Keyed (ASK) signaling. P_E for PRK is about 3 db better than that of coherent ASK or FSK. For noncoherent ASK and FSK, the probability of error is $\frac{1}{2}e^{-\frac{Z}{2}}$.

Figure 3.7 shows probability of error plots for some different binary signaling methods for comparison.

$$\begin{aligned}
\text{Var}(n_1(t)) &= E\{n_1^2(t)\} \\
&= \int_0^T \int_0^T E\{n(t)\cos(\omega_c t)n(\sigma)\cos(\omega_c \sigma)\} dt d\sigma \\
&= \int_0^T \int_0^T \cos(\omega_c t)\cos(\omega_c \sigma)E\{n(t)n(\sigma)\} dt d\sigma \\
&= \int_0^T \int_0^T \cos(\omega_c t)\cos(\omega_c \sigma)\frac{1}{2}N_0\delta(t-\sigma) dt d\sigma \\
&= \int_0^T \frac{1}{2}N_0\cos(\omega_c^2 \sigma) d\sigma,
\end{aligned}$$

where $\omega_c \sigma = x$ and $T = \frac{2\pi}{\omega_c}$

$$= \frac{1}{2} \int_0^{\omega_c T} \frac{1}{\omega_c} \cos^2 x dx$$

$$\text{Then } \text{Var}(n_1(t)) = \frac{1}{2}N_0\left(\frac{x}{2} + \frac{\sin(2x)}{4}\right)\Big|_0^{\omega_c T}.$$

Since $T = \frac{2\pi}{\omega_c}$,

$$\text{Var}(n_1(t)) = \frac{1}{2}N_0\left(\frac{T}{2} + \frac{\sin 2\omega_c \frac{2\pi}{\omega_c}}{4}\right) \text{ and it follows that}$$

$$\text{Var}(n_1(t)) = \frac{1}{4}N_0T.$$

Figure 3.6- Noise variance calculations

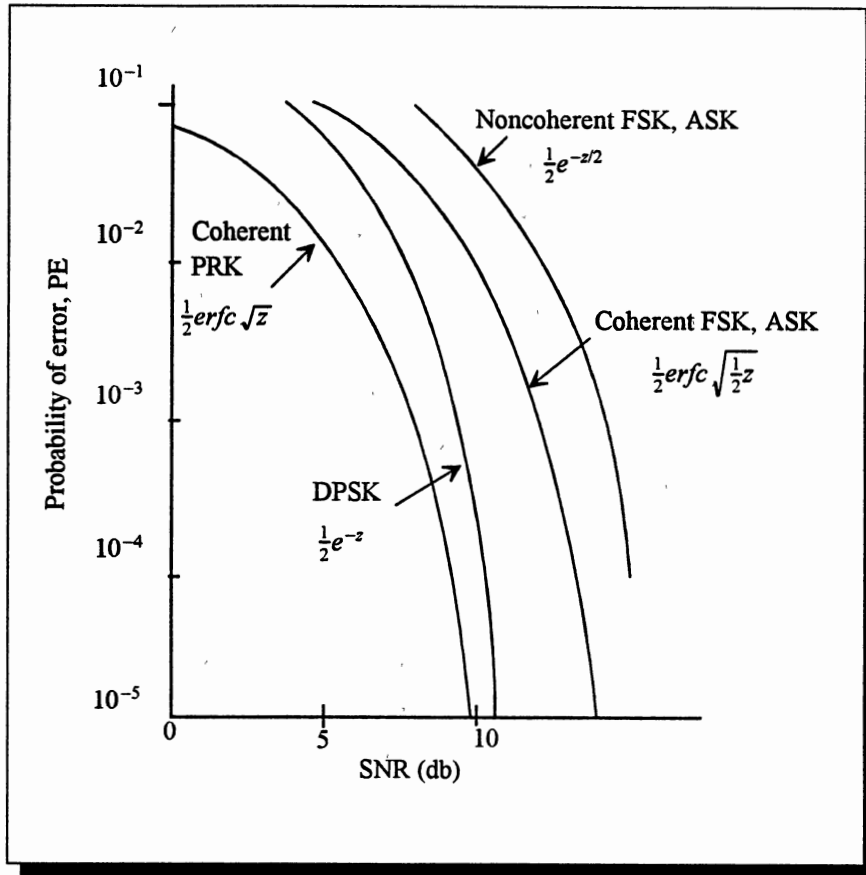


Figure 3.7- Error probabilities for some digital signaling methods

CHAPTER IV

SYSTEM OVERVIEW

The communication system under development consists of a surface receiver/transmitter pair and a downhole receiver/transmitter pair. Availability of large amounts of power for the surface transmitter and much less noise downhole relaxes the requirement for a sophisticated downhole receiver. However, the surface receiver needs a good noise cancelling system due to large amounts of surface noise. Signal processing techniques such as nonlinear processing, integration and adaptive noise cancellation can improve the Signal-to-Noise Ratio (SNR) to an acceptable level. Primary origins of Extremely Low Frequency (ELF) noise are thunder storms [12] and lightning.

Experimental data show that noise in the earth is contained mostly in the upper two thousand feet of the earth's crust. Almost all of the 60 Hz noise and its harmonics, switching noises, impulsive thunderstorm noise and other noise flow in this upper layer of earth. This is largely due to the skin effect and the high attenuation rates of electromagnetic signals in the earth.

The downhole transmitter is battery operated and has a limited output power. As the transmitter is lowered into the well, the signals received on the surface get weaker and weaker. The signal attenuation rate depends on the earth's conductivity, signal frequency and depth. Experimental data from a test well and the results obtained by Starke [9]

show through the earth attenuation rates of 5 to 10 db per thousand feet in open hole and up to 16 db per thousand feet inside metal casing for signal frequencies ranging from 3 to 20 Hz. A carrier frequency range of .2 to 20 Hz was selected based on the low background noise in that region and the signal attenuation rates.

Conventional signal processing techniques assume that the signal degradation is a known time invariant quantity. They operate as an open-loop system where no attempt is made to correct for varying noise conditions. For most geophysical signal processing systems such as EBT, the amount and type of noise varies with time and location. This is due to the varying surface conditions and the lithology of the earth. A suitable filtering technique for such operations is one which adjusts its own parameters as conditions change. This type of filter is called an adaptive filter. Adaptive processors operate in a closed-loop fashion where the output of the system is used to correct the filter parameters as the disturbances change. The input signal is filtered and compared against a desired, conditioning or training reference signal. The comparison yields an error measure $\epsilon(n)$. This error is then used to adjust the filter parameters so that $\epsilon(n)$ is progressively minimized. For most real time operations the Least Mean Square (LMS) gradient search is used to minimize the error because of its fast settling time.

Because of the very long wavelengths involved, ELF noise is highly correlated within a radius of a few miles. This fact makes the use of an adaptive noise canceller possible. Primary input to the noise canceller is derived from antennas connected to the well head. The secondary input is a reference antenna placed away from the well and not connected to the well head. This is a suitable arrangement, since the ELF noise is highly correlated

at sites separated by as much as a few miles. Also, by not having the reference antenna connected to the well head, it is ensured that minimal amounts of the EBT signal exist in the reference.

The primary input is the sum of two antennas at an angle of 180° as shown in Figure 4.1. The antenna signals are first passed through a transimpedance amplifier stage and then summed. The result is then filtered for anti-aliasing and digitized. Two antennas are used for the primary in order to cancel the effect of the impulsive noise that may be present. The well provides a path of low resistance for signals propagation. However, the impulses have equal amplitudes in the two antennas and can be canceled by summing the signals. Other signals will not be cancelled because of their direction of flow, as shown in Figure 4.2. Signals from the wellbore flow from the well head to the ground rods whereas the impulsive noise flows from the ground rod to the well head in one antenna and from the well head to the ground rod in the other.

The change in SNR depends on noise conditions. In the presence of a large amount of impulsive noise, the SNR is usually increased using the summer as compared to a single antenna configuration. This increase is the result of impulse cancellation. A decrease in SNR is possible if one of the antennas has a higher SNR relative to the other and impulsive noise is minimal. The following calculations show how the SNR can be increased by the sum when the noise is the same in the two primary antennas.

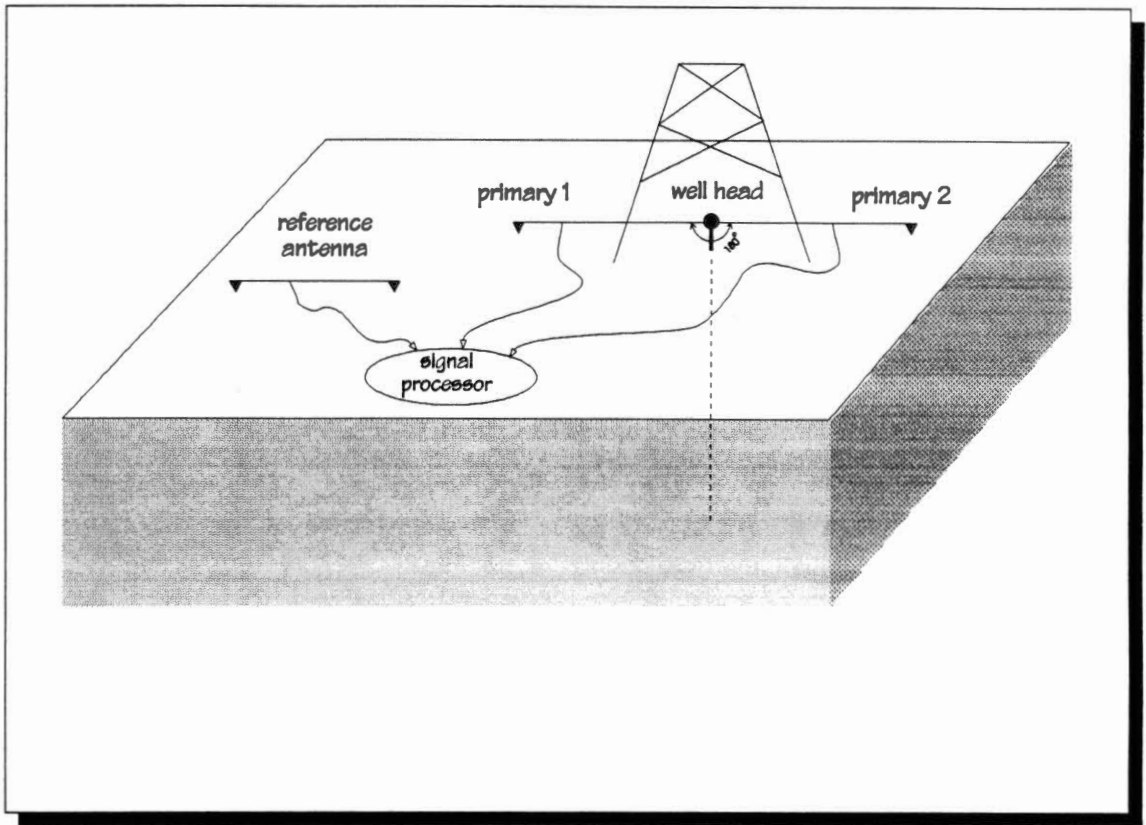
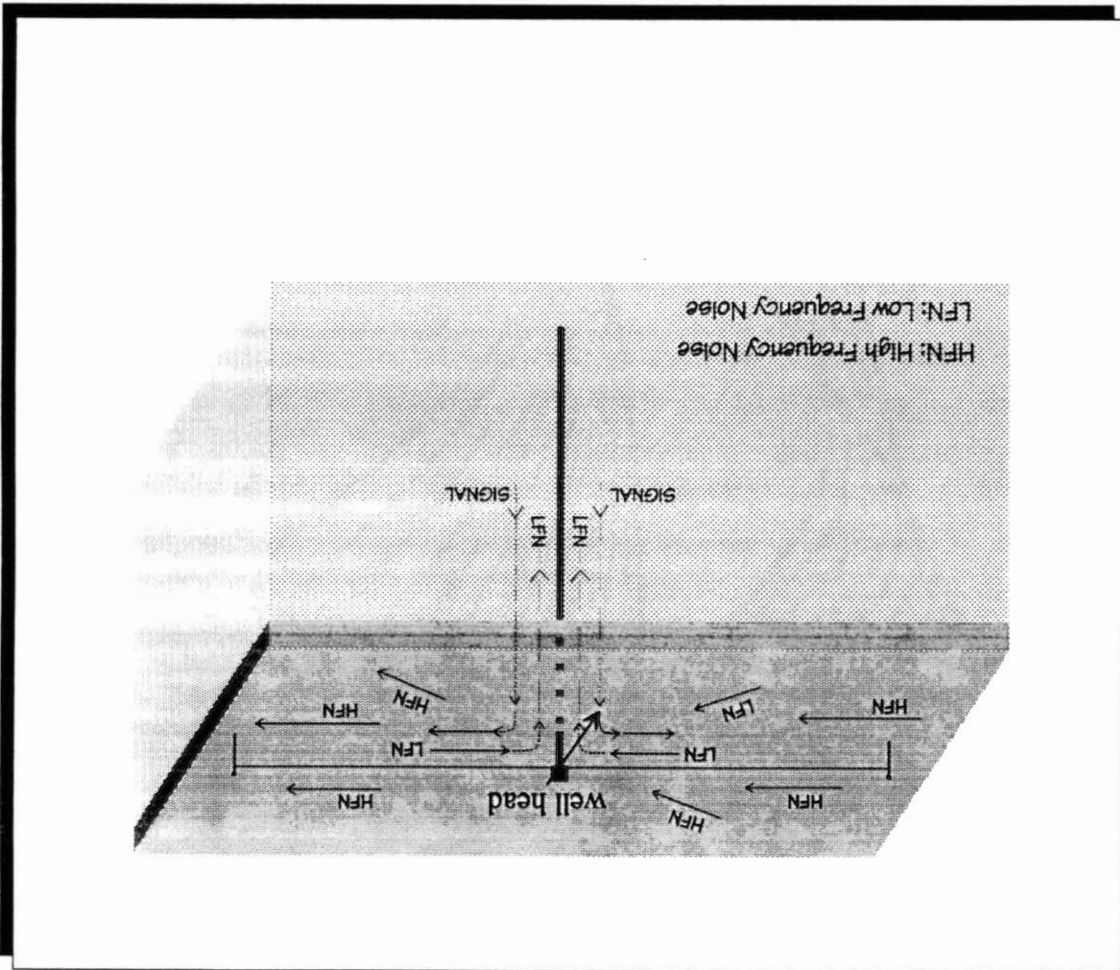
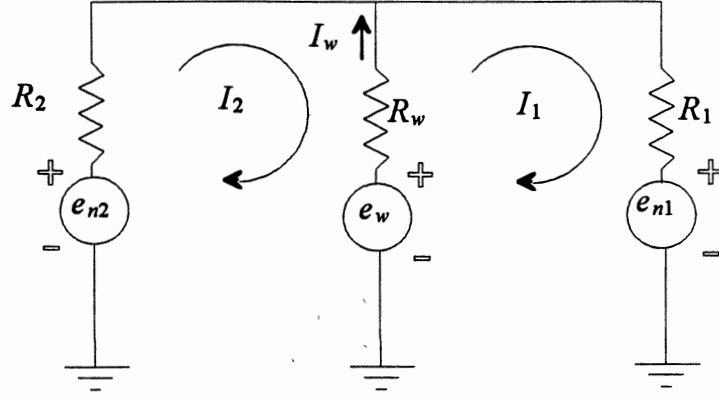


Figure 4.1- Antenna arrangement

Figure 4.2- Current flow directions in the earth





Each of the primary antenna wires is connected at one end to the well head and at the other end to a ground rod buried in the earth. Voltage induced in the antennas are labeled as e_{n1} and e_{n2} with antenna resistances as R_1 and R_2 . The downhole transmitter antenna voltage and resistance are labeled e_w and R_w . Writing the mesh equations results in

$$-e_w + R_w(I_1 - I_2) + I_1 R_1 + e_{n1} = 0 \quad (4.1)$$

$$-e_{n2} + I_2 R_2 + R_w(I_2 - I_1) + e_w = 0 \quad , \quad (4.2)$$

and subsequently

$$I_1(R_1 + R_w) - R_w I_2 + e_{n1} - e_w = 0 \quad (4.3)$$

$$I_1(-R_w) + I_2(R_w + R_2) + e_w - e_{n2} = 0 \quad (4.4)$$

solving for I_1 provides

$$I_1 = \frac{e_{n1} - e_w + R_w I_2}{R_1 + R_w} \quad (4.5)$$

$$\frac{e_{n1} - e_w + R_w I_2}{R_1 + R_w} (-R_w) + I_2(R_w + R_2) + e_w - e_{n2} = 0 \quad . \quad (4.6)$$

since $I_w = I_1 - I_2$

$$I_1 = \frac{-R_w e_{n1} + R_2 e_w - R_2 e_{n1} + R_w e_{n2}}{R_1 R_w + R_1 R_2 + R_2 R_w} \quad (4.7)$$

and

$$I_2 = \frac{-R_w e_{n1} + R_1 e_{n2} - R_1 e_w + R_w e_{n2}}{R_1 R_w + R_1 R_2 + R_2 R_w} \quad , \quad (4.8)$$

therefore

$$I_w = \frac{(R_1 + R_2) e_w - R_1 e_{n2} - R_2 e_{n1}}{R_1 R_w + R_1 R_2 + R_2 R_w} \quad . \quad (4.9)$$

In the case where ground rods have the same resistance

$R_1 = R_2$ and

$$I_w = \frac{2e_w(e_{n1}+e_{n2})}{2R_w+R_1} \quad (4.10)$$

for this case,

$$SNR = \frac{2e_w}{\sqrt{e_{n1}^2+e_{n2}^2}} \quad (4.11)$$

and if noise sources in the two antennas are of the same magnitude,

$$SNR = \frac{2e_w}{\sqrt{2} e_n} = \sqrt{2} \frac{e_w}{e_n} = \sqrt{2} SNR_{\text{one rod}} \quad (4.12)$$

The result is an increase in SNR by a factor of $\sqrt{2}$ for two antennas. Generally, for N antennas with equal ground rod resistances, the SNR is improved by factor \sqrt{N} . Plots of data available to the primary input and the secondary input, as well as the data transmitted through the borehole is shown in Figures 4.3 and 4.4. Figure 4.5 shows the time and frequency domain representations of a simulated borehole signal similar to the signal transmitted in Figures 4.3 and 4.5.

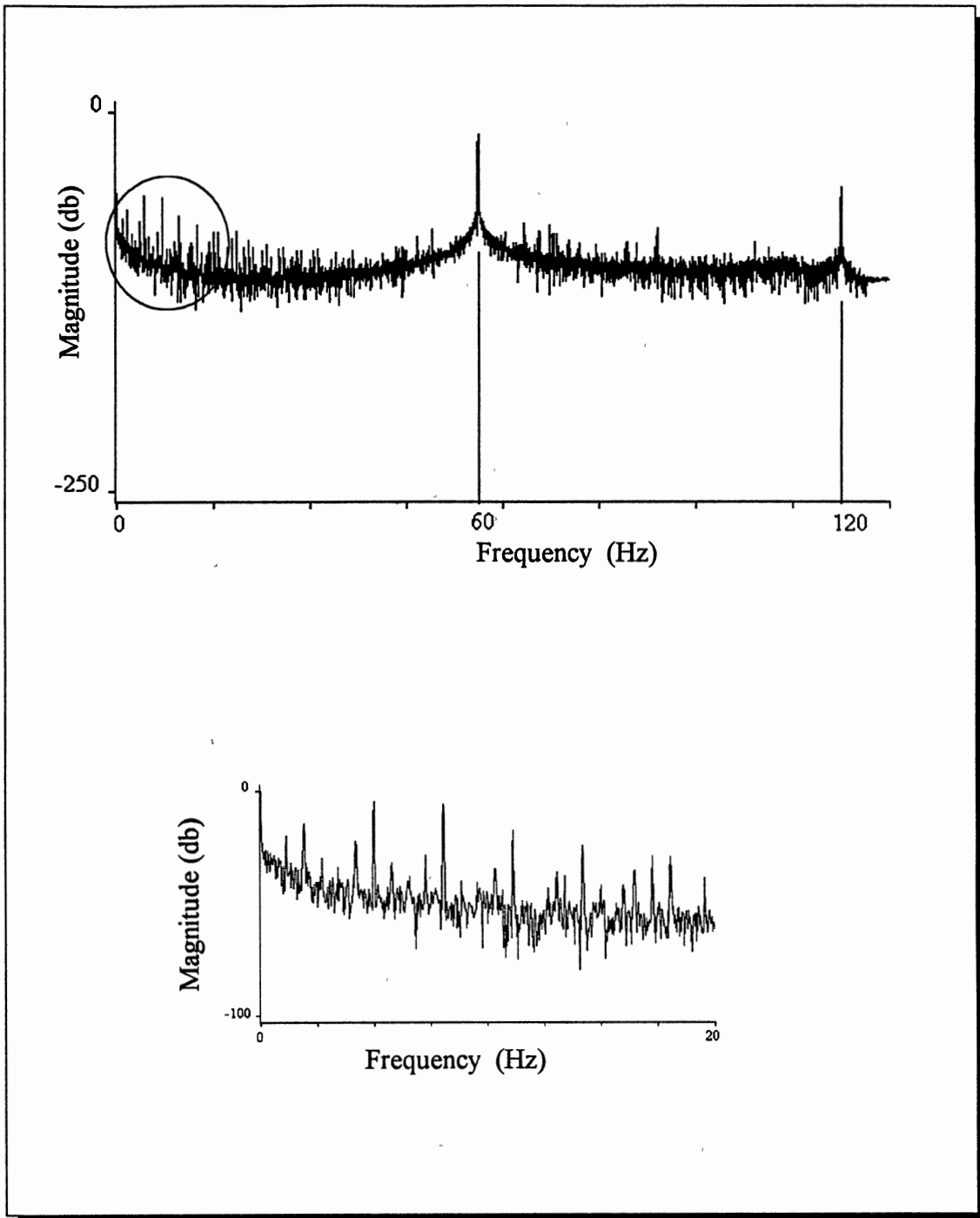


Figure 4.3- Primary input spectrum containing PRK modulated 6 Hz signal

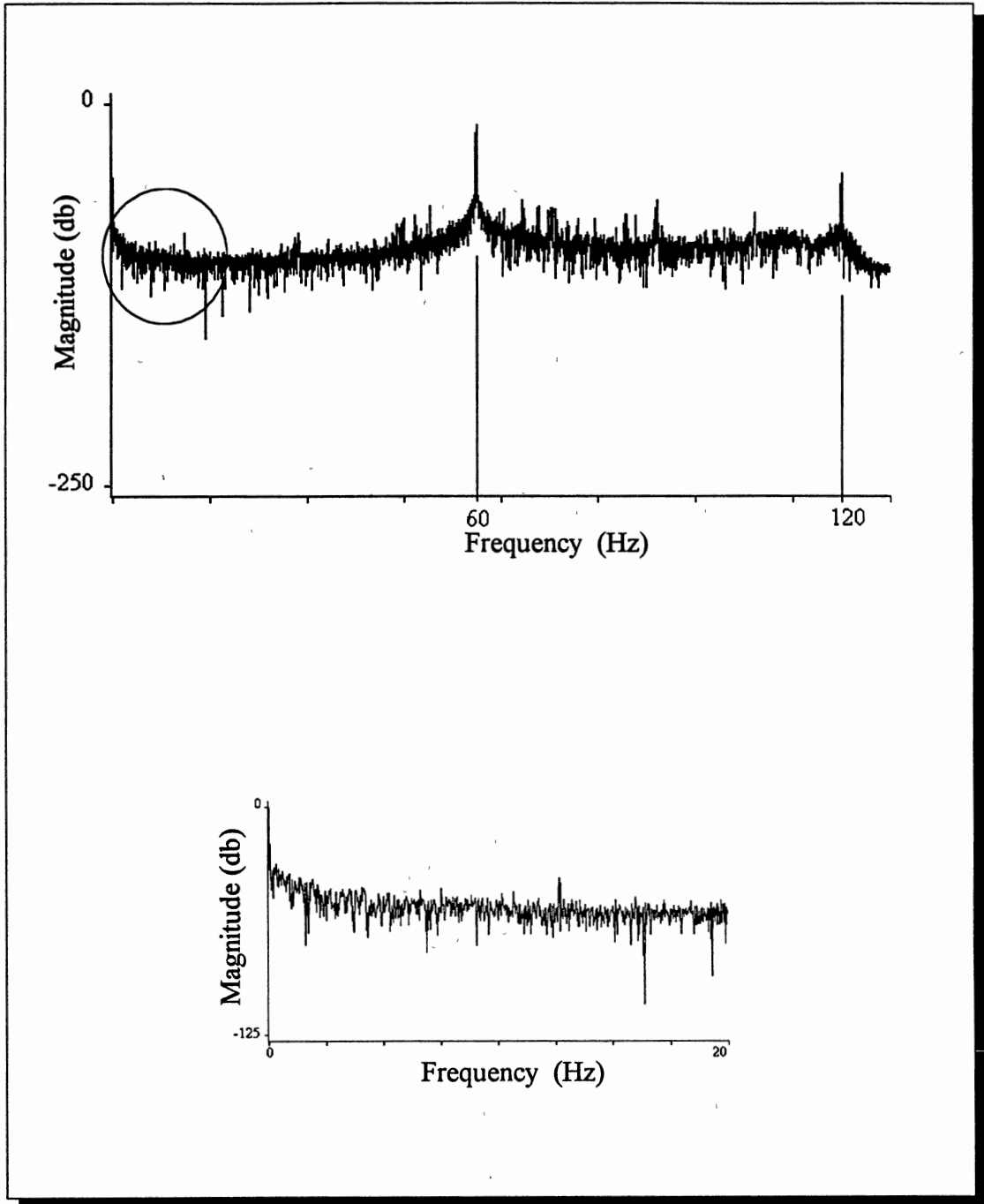


Figure 4.4- Reference input spectrum containing only noise

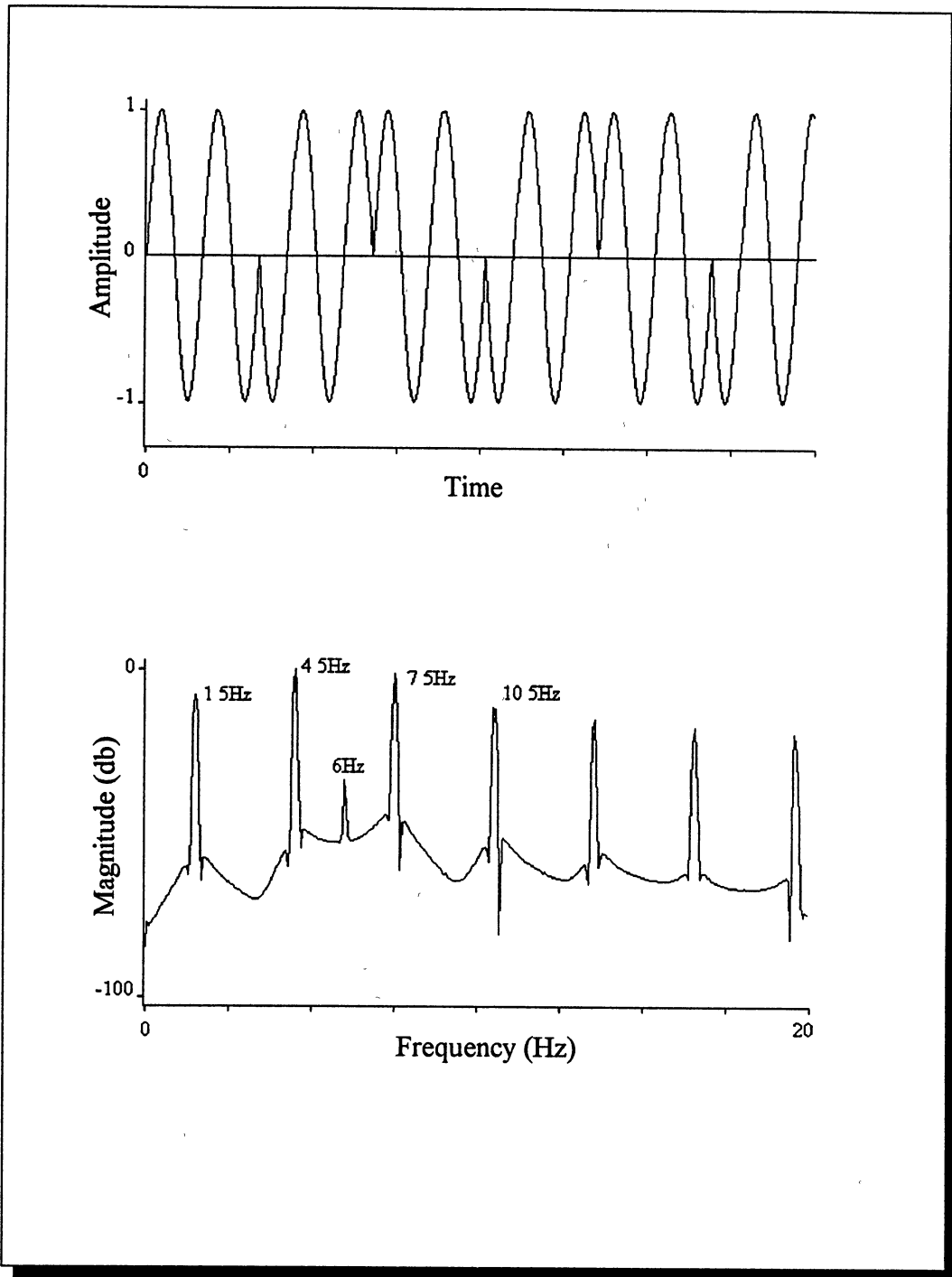


Figure 4.5- Simulated 6Hz signal

The Block diagram of the complete signal processing system is shown in Figure 4.6. The antenna signals are first routed through an analog receiver. The analog receiver consists of three major stages. The first stage is a radio frequency filter which rejects the high frequency signals picked up by the antennas. The second stage is a summer which sums the two primary antenna signals for impulsive noise reduction. The bandwidth of the analog receiver is from 0.03 Hz to 139 KHz which is due to the use of dc servos to remove dc components for better dynamic range and the rf filters. The final stage is a low pass antialiasing filter stage which prepares the signals for digitization. The rest of the processing is digital.

The First step of digital signal processing is passing the reference input through an impulsive noise removal stage in preparation for adaptive filtering. This stage is necessary when impulses are present since a reference input containing impulsive noise to the adaptive filter can distort the output significantly. The primary input does not require this stage since the analog summing process will remove the majority of the impulses from the data. The block diagram of the impulse removal stage was shown in Figure II 12 and its operation is explained in the impulsive noise removal section. The adaptive filter parameters are μ and N_w , μ determines the speed of convergence and N_w is the number of weights or tabs used. The values of these parameters were chosen for quickest convergence time and maximum noise cancelling effect.

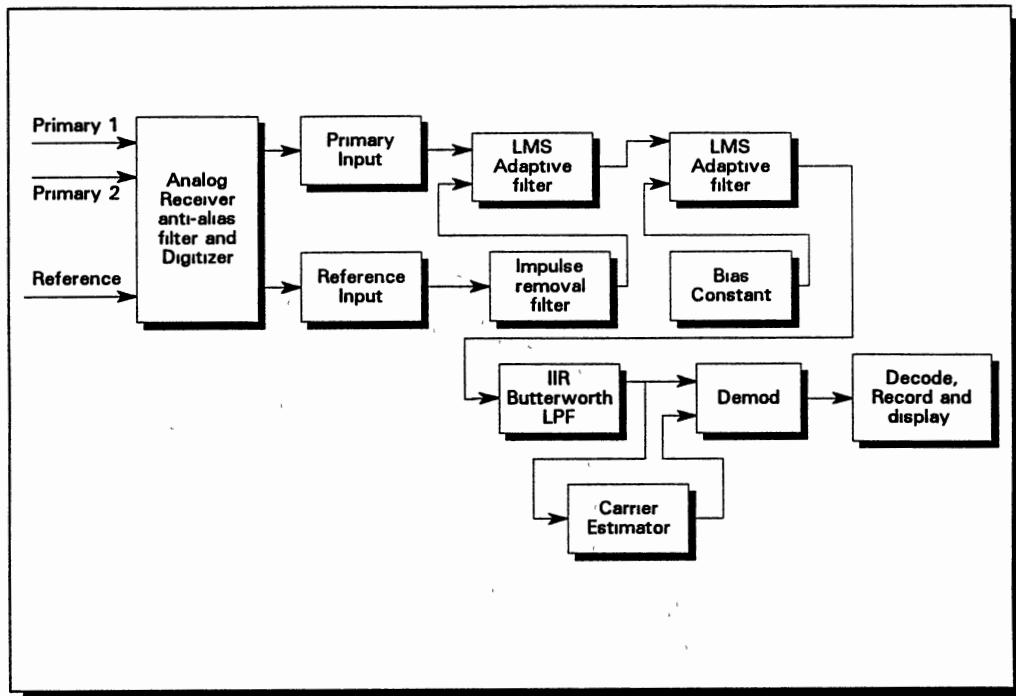


Figure 4.6- EBT Signal Processor

CHAPTER V

SUMMARY AND CONCLUSIONS

This thesis has presented a problem of borehole communications for oil well operations together with part of the solution. The part of the solution presented consists of the surface digital data processing system for the communications system.

What is different about this signal processing application is the frequency range of the signals involved. The signals are transmitted within an extremely low frequency range. Signal processing in the ELF range requires large blocks of data for processing and special filtering system to remove the noise in that range. The wide input band requires high sampling rates compared to the frequency of the transmitted signals. This comparatively high sampling rate and the low signal frequencies warrant the need of large blocks of data.

The type of noise present in the ELF band is unique in that low frequency noise travels further and it can originate from distant and difficult to model sources. The level of noise present in the earth varies with location and the weather conditions. The noise level increases as one moves inside the power grid and also when the weather is stormy and specially when lightning strikes around the operations area. Lightning strikes can produce large spikes in the data.

An impulsive noise canceller system was presented which benefitted the low sample rate data by removing spikes using frequency domain threshold filtering. The major noise

cancellation is accomplished by using an adaptive noise canceller. Primary input to the adaptive noise canceller comes in as the sum of outputs of two wire antennas connected to the well head. The summing operation provides some impulsive noise cancellation. For the impulses which pass through the summer, additional cancellation is required.

Reference signal comes from a separate wire antenna which is stretched between two ground rods. The reference antenna provides the adaptive noise canceller with data that contains highly correlated noise to that of the primary. Adaptive noise canceller functions by estimating the noise contained in the primary using the reference data and it then subtracts that estimate from the primary signal. The power grid noise, any on location equipment electrical noise in the earth, and the ELF noise all exist in both the primary and the reference antennas and are highly correlated.

A modulation/demodulation system was selected which provides the smallest bit error rate for this application. Due to the difficulty of obtaining a coherent carrier, a differential modulation system was chosen. The DPSK system compares the phase of one cycle with that of the previous cycle and decisions are based on the relative phases of the cycles, the first one being a reference with a known phase. An alternative demodulation system based on a backpropagation neural network was also discussed and results of simulations were presented. The results indicate the potential of neural networks for such applications.

In conclusion, a surface receiver digital signal processing system has been designed which enables the communications system to operate successfully to a depth of 3000 feet in casing and over 5000 feet in open hole. The downhole transmitter operates at 4 amperes rms at 3Hz, using a series of rechargeable batteries. As the transmitter is lowered

deeper in the borehole, the signals received on the surface begin to fall below the earth's noise floor and the signal-to-noise-ratio falls below useful levels. More than 4 amperes rms output is needed in order to be able to extract the signals of interest at deeper depths on the surface. A few decibels could probably be gained by using redundant coding which would slow down the transmission rate. Larger gains however, can only be gained by employing a more powerful downhole power system. For example, a mud turbine power generator which produces power in orders of hundreds of watts could be employed in situations where drilling mud is flowing in the borehole.

Suggestions for future work

The recommended future work in this area would be work on a nonredundant coding scheme for error detection and correction which is highly desirable because of the already low data rates. Further research on the use of neural networks in signal filtering and demodulation. For a brief treatment of the backpropagation neural network, see appendix Theoretical analysis of neural network systems and a good performance measure in their use as demodulators would be a good subject for future research. And finally a better power system for such applications. Due to the size and other restrictions set upon the EBT system, batteries must be used as the power source and more compact and powerful batteries would be highly desirable for such applications. Having available more power to the borehole transmitter, higher data rates can be achieved by using either higher carrier frequencies or different modulation schemes such as m-ary phase shift keyed modulation.

Obviously a compromise between modulation method and carrier frequency must be made in order to the best results for an optimum borehole data communication system.

REFERENCES

- [1] B. Widrow, S. D. Stearns, *Adaptive Signal Processing*, New Jersey: Prentice-Hall, 1985.
- [2] R. E. Zimmer, W. H. Tranter, *Principles of Communications, Systems, Modulation, and Noise*, Boston: Houghton Mifflin, 1990.
- [3] W. C. Lindsey, "Phase-Shift-Keyed Signal Detection with Noisy Reference Signals", *IEEE Trans. on Aerospace and Electronic Systems*, Vol. AES-2, No. 4, pp. 393-401, July 1966.
- [4] R. Haeb, "A Comparison of Coherent and Differentially Coherent Detection Schemes for Fading Channels", *IEEE International Conference on Communications*, pp. 364-370, Sep. 1988.
- [5] N. C. Gallagher Jr., G. L. Wise, "A Theoretical Analysis of the Properties of Median Filters", *IEEE Trans. Acoustics, Speech, and Signal Processing*, Vol. ASSP-29, No. 6, pp. 1136-1141, December 1981.
- [6] R. Desbrandes, "Status Report: MWD Technology, part 1", *Petroleum Engineering International*, pp. 27-33, Sep. 1988
- [7] R. Desbrandes, "Status Report: MWD Technology, part 2", *Petroleum Engineering International*, pp. 48-54, Oct. 1988
- [8] R. Desbrandes, "Status Report: MWD Technology, part 3", *Petroleum Engineering International*, pp. 42-51, Nov. 1988.
- [9] D. B. Starkey, "Electromagnetic Transmission at Deep Depths", *Acceptance Technology Division of Sandia Laboratories in Livermore*, pp. 140-175, 1988.
- [10] B. Widrow, J. R. Glover Jr., J. M. McCool, J. Kaunitz, C. S. Williams, R. H. Hearn, J. R. Zeidler, E. Dong Jr., R. C. Goodlin, "Adaptive Noise Cancelling: Principles and Applications", *Proceedings of the IEEE*, Vol. 63, No. 12, pp. 1692-1716, Dec. 1975.

- [11] R. G. Geyer, G. V. Keller, "Constraints Affecting Through-the-Earth Electromagnetic Signalling and Location Techniques", *Radio Science*, Vol. 11, No 4, pp. 323-342, April 1976.
- [12] F. H. Raab, "Signal Processing for Through-the-Earth Electromagnetic Systems", *IEEE Trans. on Industry Applications*, Vol. 24, No. 2, pp. 212-216, March/April 1988.
- [13] F. H. Raab, "Adaptive Noise Cancellation Techniques for Through-the-Earth Electromagnetics, volume II", *Final Report GMRR TR82-1, Green Mountain Radio Research Company*, Winooski, VT, Jan. 1982.
- [14] A. D. Spaulding, D. Middleton, "Optimum Reception in an Impulsive Interference Environment-Part I: Coherent Detection, Part II: Incoherent Reception", *IEEE Trans. on Communications*, Vol. COM-25, No. 9, pp. 910-934, Sep. 1977.
- [15] M. Kato, H. Inose, "DDM Differentially Coherent Detection of DPSK Signals", *Electronics and Communications in Japan*, Vol. J59-A, No. 2, pp. 40-50, 1976.
- [16] J. H. Winters, "On Differential Detection of M-ary DPSK with INtersymbol Interference and Noise Correlation", *IEEE Transactions on Communications*, Vol. COM-35, No.1, pp.117-120, January 1987.
- [17] J. B. Allen, L. R. Rabiner, "A Unified Approach to Short-Time Fourier Analysis and Synthesis", *Proceedings of the IEEE*, Vol. 65, No. 11, pp. 1558-1564, Nov 1977
- [18] S. Samejima, K. Enomoto, Y. Watanabe, "Differential PSK System with Nonredundant Error Correction", *IEEE Journal on Selected Areas in Communications*, Vol. SAC-1, No. 1, pp. 74-81, Jan. 1983
- [19] A. Papoulis, *Probability, Random Variables, and Stochastic Processes*, McGraw-Hill, 1965.
- [20] A. V. Oppenheim, R. W. Schaffer, *Digital Signal Processing*, New Jersey. Prentice-Hall, 1975.
- [21] S. Samejima, "Differential PSK System with Nonredundant Error Correction", *IEEE Journal on Selected Areas in Communications*, Vol. SAC-1, No. 1, pp. 74-81, January 1983.
- [22] H. Bode and C. Shannon, "A Simplified Derivation of Linear Least Squares Smoothing and Prediction Theory", *Proc. IRE* Vol. 38, pp 417-425, Apr.1950
- [23] M. Gearhart, L.M. Moseley and M. Foster, "Current State of the Art of MWD and Its Application in Exploration and Development Drilling", *SPE 14071* , March 1986

- [24] M. Gearhart, K.A. Ziemer and O.M. Knight, "Mud Pulse MWD (Measurement-While-Drilling) Systems", *SPE 10053*, October 1981.
- [25] F.W. LeGros Jr., C.A. Martin, "Applications of Measurements While Drilling (MWD): Development of the East Breaks Field, Offshore Texas", *SPE/IADC 13487*, March 1985.
- [26] W.H. Harrison, R.L. Mazza, L.A. Rubin and A.B. Yost II, "Air-Drilling, Electromagnetic, MWD System Development", *IADC/SPE 19970*, February 1990.
- [27] G. Lafont, "Telemetry System Incorporating Synchronization of Receiver with Transmitter", *U.S. Patent No. 3,707,700*, Dec. 26, 1972.
- [28] J.J. Flagg, "Well Logging Data Transmission System", *U.S. Patent No. 4,415,895*, Nov. 15, 1983.
- [29] E.B. Denison, "Drill String Telemetry System", *U.S. Patent No. 4,126,848*, Nov. 21, 1978.
- [30] A.B. Beynes, A. Paumard, Y. Durand, T.J. Calvert, "Well Logging Communication System", *U.S. Patent No. 4,355,310*, Oct. 19, 1982.
- [31] A.O. Woods, "Borehole Measurement and Telemetry System", *U.S. Patent No. 4,646,083*, Feb. 24, 1987.
- [32] W.H. Cox, P.E. Chaney, "Telemetry System", *U.S. Patent No. 4,293,936*, Oct. 6, 1981.
- [32] N. Yamazaki, "Well Data Transmission System Using a Magnetic Drill String for Transmitting Data as a Magnetic Flux Signal", *U.S. Patent No. 4,800,385*, Jan. 24, 1989.
- [33] A. M. Nicolson, "Electromagnetic Wave Telemetry System for Transmitting Downhole Parameters to Locations Thereabove", *U.S. Patent No. 4,160,970*, Jul. 10, 1979.
- [34] J.R. Claycomb, "Apparatus and Method for Transmitting Downhole Conditions to the Surface", *U.S. Patent No. 4,734,893*, Mar. 29, 1988.
- [35] E. S. Mumby, "Apparatus for Well Logging Telemetry", *U.S. Patent No. 4,550,392*, Oct. 29, 1985.
- [36] R. Jurgnes, "Process and Dvice for Transmitting Information Over a Distance", *U.S. Patent No. 4,641,289*, Feb. 3 1987.

- [37] E. S. Mumby, "Apparatus for Well Logging Telemetry", *U.S. Patent No. 4,699,352*, Oct. 3, 1987.
- [38] R. H. Nielsen, *Neruo Computing*, Addison Wesley publishing Co. Inc., 1989.
- [39] J. A. Freeman, D. M. Skapura, *Neural Networks, Algorithms, Applications, and Programming Techniques*, Addison Wesley Publishing Co. Inc., 1991.
- [40] M. Caudill, "Neural Network Primer", *AI Expert*, pp. 2-64, May 1991.
- [41] R. J. Guest, "Surface Antenna/Receiver Coupling", *EBT Report, Halliburton Services*, July 24, 1991.
- [42] J. M. Richardson, "Modulated 3 and 6 Hz Tests In Casing", *EBT Report, Halliburton Services*, Dec. 5, 1991.
- [43] Louis H. Rorden, "Wireless Subterranean Signaling Method", *U. S. Patent No. 3,967,201*, June 29, 1976.
- [44] Mario D. Grossi, Robert K. Cross, "Electromagnetic Lithosphere Telemetry System", *U. S. Patent No. 4,087,781*, May 2, 1978.
- [45] Arnold J. Farstad, Carl Fisher Jr., "Wireless FSK Technique for Telemetering Underground Data to the Surface", *U. S. Patent No. 4,090,135*, May 16, 1978.
- [46] B. Widrow and M. Hoff, Jr., "Adaptive Switching Circuits", in *IRE WESCON conv. Rec.*, pt. 4., pp. 96-104, 1960.
- [47] E. D. Chesmore, "Application of Pulse Processing Neural Networks in Communications and Signal Demodulation", *First IEE International Conference on Artificial Neural Networks*, Lindon, Engl , pp. 337-341, Oct 16-18, 1989.
- [48] E. D. Chesmore, "A Connectionist Architecture for Signal Demodulation in Communication Systems", *Second Bangor Symposium on Communications*, pp. 163-166, May 23-24, 1990.

APPENDIX

NEURAL NETWORKS

This appendix is very concise and is not meant to be a comprehensive treatment of neural networks. For those interested in a detailed tutorial, see [38],[39] and [40].

According to J.A. Freeman and D.M. Skapura [38], the neural network structure is defined as a collection of parallel processors called nodes or processing elements connected together in the form of a directed graph, organized such that the network structure lends itself to the problem being considered. It is a new approach to information processing that does not require algorithm or rule development and often reduces the quantity of the software required. The neural network can autonomously develop operational capabilities in adaptive response to an information environment. The parallel architecture of neural networks makes them extremely useful in pattern recognition applications. Signal demodulation can be considered to be a pattern recognition application.

There are many different neural network architectures, such as Backpropagation networks, Kohonen networks, counter propagation networks and others. We are concerned here with the Backpropagation networks. Backpropagation is a gradient descent algorithm that tries to minimize the average squared error of the network by moving down the gradient of the error curve. This type of network consists of multiple

layers of processing elements with each layer connected to the ones immediately above and below it and there are no connections between the nodes on a layer. An example of a three layer Backpropagation network is shown in Figure A.1. The input layer is a fan-out layer with each node having a single input and multiple outputs. On the other layers, each processing element has a number of input signals and a single output signal as shown in Figure A.2. Each input signal, x_i , is assigned a weight, w_i . The total input for each processing element is the summation of all inputs multiplied by their corresponding weights. The output of each processing element is normally determined using a nonlinear function such as the sigmoid function which is an S shaped curve which asymptotically approaches constants. This non linear function is called the activation function and it determines whether the particular processing element fires. The reason for using the sigmoid function is that it is differentiable, it approaches fixed values asymptotically and it is monotonically increasing. The first condition is important because the function is differentiated in the learning process and the other conditions are important for binary outputs.

The first step in the design of a neural net system, after the basic architecture is selected, is the training process. A neural net system must first "learn" how to react to a given input vector. During this process many input vectors representing what might be encountered in run time are introduced to the network. The network learns or adjusts its parameters by comparing its output with the known outputs. The comparison yields error values that are propagated back through the network and that are used to adjust the weights according to the Least Mean Squared (LMS), or Delta, learning rule. The LMS

learning rule is similar to the one used in adaptive filtering and noise cancelling. This is an iterative process which will end when the output errors are reduced to an acceptable level, Figure A.3.

The learning process starts where the training patterns are fed to the input layer of the network. From there they are fanned out to the middle layer. The middle layer processing elements process the inputs and pass the results to the next layer,

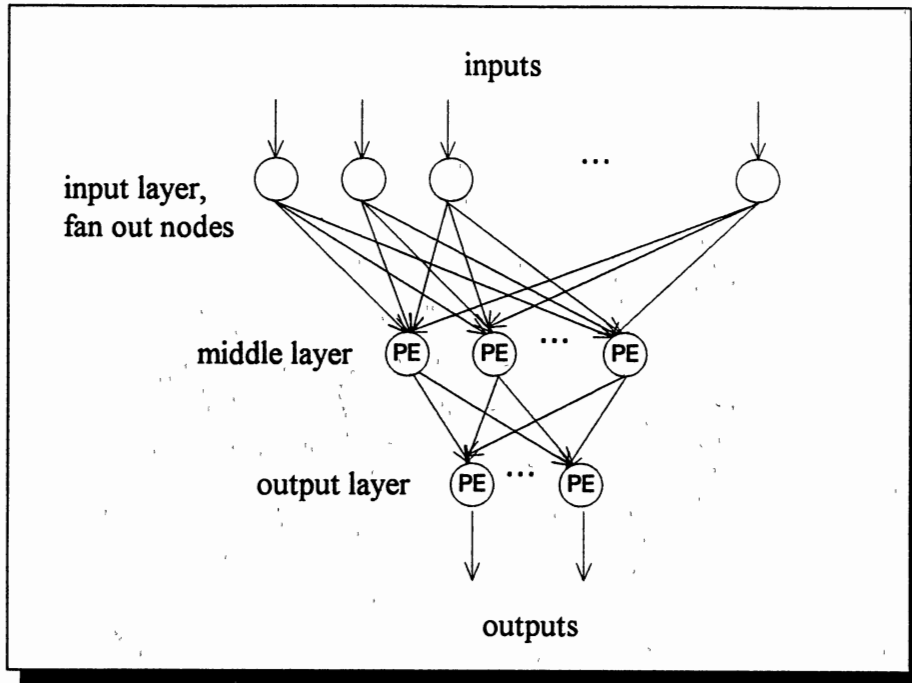


Figure A.1- Backpropagation neural network architecture.

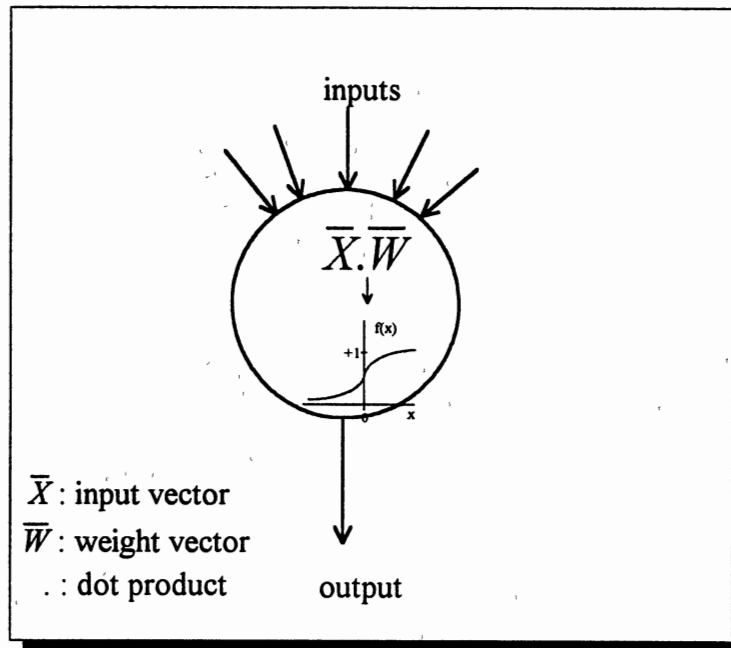


Figure A.2- A Processing Element (PE)

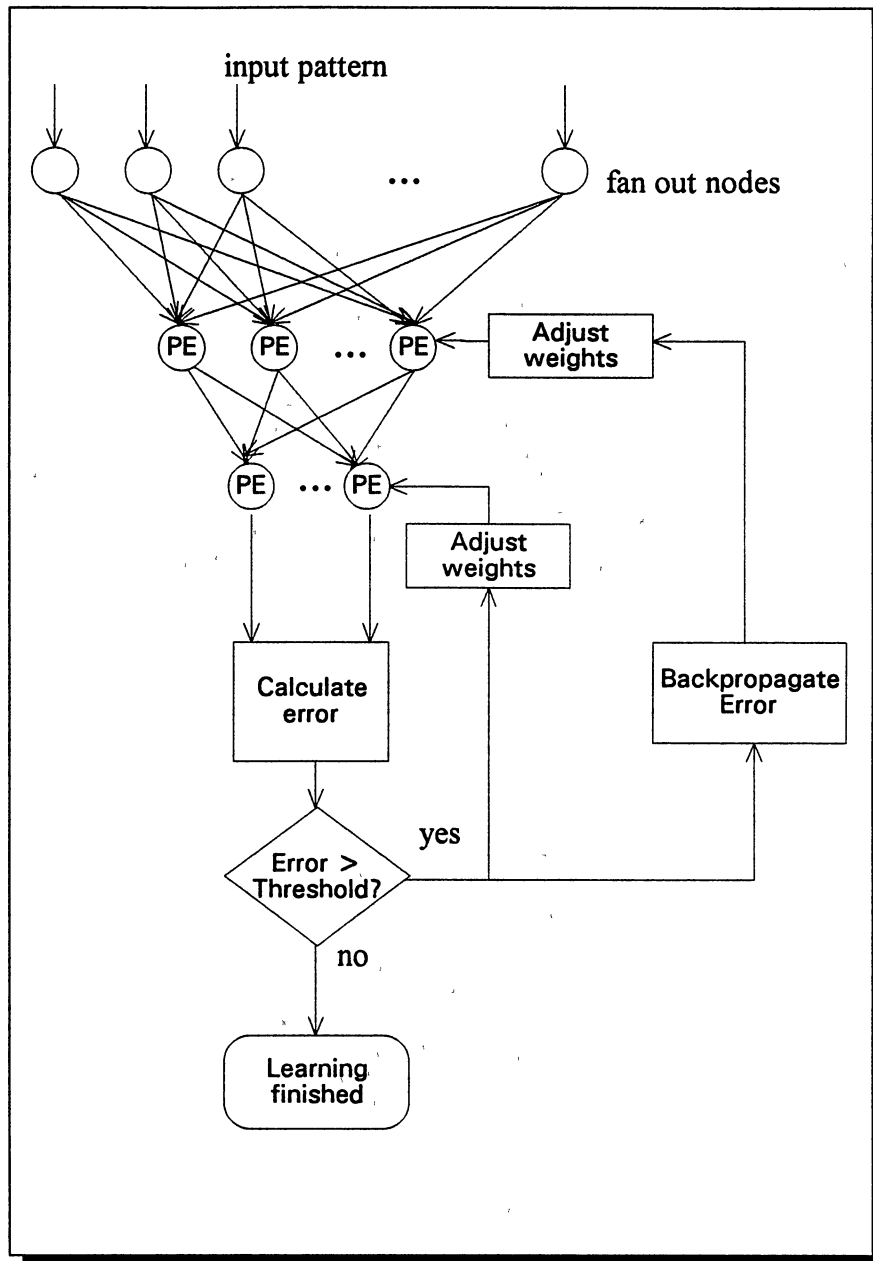


Figure A.3- Learning process in a three layer backpropagation neural network.

$$I = \bar{X} \cdot \bar{W} \quad (A.1)$$

or $I = \sum x_i w_i$

\bar{X} and \bar{W} are the input and weight vectors. The output of the PE becomes,

$$f(I) = \frac{1}{1+e^{-I}} \quad \text{The Sigmoid function} \quad (A.2)$$

After the outputs for the last layer are calculated, they are compared to the desired values.

The difference is used to update the weights. The update follows the Delta rule:

$$\bar{W}_{new} - \bar{W}_{old} = \frac{\beta E \bar{X}}{|\bar{X}|^2} \quad (A.3)$$

for each PE, where β is the learning constant and E is an error value calculated by subtracting the output from the desired value for the output layer. This same value is propagated back to previous layers. The backward propagation is performed as

$$e = f'(I) [\sum w_{ij} E_j] \quad (A.4)$$

where i is the input index, j is the PE index and

$$f'(x) = \frac{d}{dx} \left(\frac{1}{1+e^{-x}} \right) \quad (A.5)$$

$$= \frac{0 - (-e^{-x})}{(1+e^{-x})^2} \quad (A.6)$$

$$= \frac{e^{-x}}{(1+e^{-x})} \quad (A.7)$$

Factoring $f(x) = \frac{1}{1+e^{-x}}$ results in

$$f'(x) = f(x)[1 - f(x)] \quad (A.8)$$

f' serves as a stabilizing factor since it is a bell shaped curve with relatively large values for mid-range inputs and smaller values for either end. This helps in convergence of the

system since it forces the changes to be small when the outputs approach 0 and 1, with larger changes otherwise.

One important addition to the Delta rule is the momentum term. The momentum term helps to keep the weight changes going in the same direction and to keep the solution out of the local minima. The rule incorporating this additional term is called the generalized Delta rule,

$$\bar{W}_{new} = \bar{W}_{old} + \frac{\beta E \bar{x}}{|\bar{x}|^2} + \alpha(\bar{W}_{new} - \bar{W}_{old})_{prev} \quad (A.9)$$

where α is the constant momentum term multiplied by the change in weights for this node from the previous iteration.

VITA

Farhad Esfahani

Candidate for the Degree of

Doctor of Philosophy

**Thesis: EXTREMELY LOW FREQUENCY (ELF) SIGNAL PROCESSING FOR
ELECTRIC BOREHOLE TELEMETRY**

Major Field: Electrical Engineering

Biographical

Personal Data: Born in Tehran, Iran, June 21, 1961, the son of Ali Esfahani and Parivash Nameni Esfahani.

Education: Graduated from Lincoln High School, Seattle, Washington in May 1980, received the Bachelor of Science degree in Electrical Engineering from Oklahoma State University in May 1984; received the Master of Science degree in Electrical Engineering from Oklahoma State University in May 1986; completed requirements for the Doctor of Philosophy degree at Oklahoma State University in December 1992.

Professional Experience: Senior Engineer, Halliburton Services Company Research Center, June 1989 to present; graduate research assistant, School of Electrical and Computer Engineering, Oklahoma State University, August, 1987, to May, 1989; lab instructor, School of Electrical and Computer Engineering, Oklahoma State University, August, 1986, to May 1987.

Awards/Affiliations: Member Tau Beta Pi, Eta Kappa Nu, Institute of Electrical and Electronics Engineers (Communications Society, Neural Networks Society and Computer Society). Member Kiwanis International